AMERICAN UNIVERSITY OF BEIRUT

JOINT PROCESSING COORDINATED MULTIPOINT THROUGH RELAYING AND LESS BS INVOLVEMENT

by
TANIA SAOUMA

A thesis
submitted in partial fulfillment of the requirements
for the degree of Master of Engineering
to the Department of Electrical and Computer Engineering
of the Faculty of Engineering and Architecture
at the American University of Beirut

Beirut, Lebanon
April 2016

AMERICAN UNIVERSITY OF BEIRUT

JOINT PROCESSING COORDINATED MULTIPOINT THROUGH RELAYING AND LESS BS INVOLVEMENT

by
TANIA SAOUMA

Approved by:

_____
Dr. Hassan Artail, Professor   Advisor
Electrical and Computer Engineering

_____
Dr. Zaher Dawy, Professor   Member of Committee
Electrical and Computer Engineering
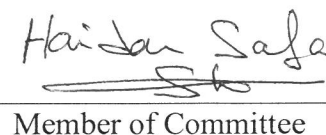
_____
Dr. Youssef Nasser, Professor   Member of Committee
Electrical and Computer Engineering

_____
Dr. Haidar Safa, Professor   Member of Committee
Computer Science

Date of thesis defense: April 21, 2016

AMERICAN UNIVERSITY OF BEIRUT

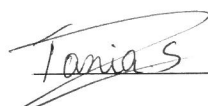# THESIS, DISSERTATION, PROJECT RELEASE FORM

Student Name: __Saouma_____Tania_____Youssef__
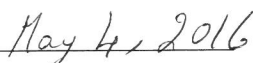   Last   First   Middle

⊗ Master's Thesis   ◯ Master's Project   ◯ Doctoral Dissertation

☐   I authorize the American University of Beirut to: (a) reproduce hard or electronic copies of my thesis, dissertation, or project; (b) include such copies in the archives and digital repositories of the University; and (c) make freely available such copies to third parties for research or educational purposes.

☒   I authorize the American University of Beirut, **three years after the date of submitting my thesis, dissertation, or project,** to: (a) reproduce hard or electronic copies of it; (b) include such copies in the archives and digital repositories of the University; and (c) make freely available such copies to third parties for research or educational purposes.

_Tania S_____   _May 4, 2016_____

Signature   Date

ACKNOWLEDGMENTS

AN ABSTRACT OF THE THESIS OF

Tania Youssef Saouma   for   Master of Engineering
                                    Major: Electrical and Computer Engineering

Title: Joint Processing Coordinated Multipoint through Relaying and Less BS Involvement

Joint processing coordinated multipoint (JP-CoMP) is a new technology in LTE-A adopted to enhance the throughput of cell edge users as well as to mitigate interference. Relay Nodes (RNs) have also proven useful toward the realization of LTE-A, in improving the signal quality for the cell edge users. In my thesis, I propose to combine JP-CoMP and relaying techniques for further improvements at the cell edge User equipment (UEs). The design exploits available RNs (fixed or mobile) in the cell coverage area, and allows them to participate in the coordination process with the base stations (BSs). To reduce the complexity burden, two BSs and two RNs are proposed to be used in the cooperating set, rather than three BSs as proposed in literature. Moreover, the optimal positions of the RNs were analyzed, and the maximum data rate was proven to be achieved at different cooperative RN locations, depending on the power ratio between the RN and the BS. The simulation results show that the proposed design improves capacity and bit error rate performance in comparison with conventional JP-CoMP. Finally, power allocation analysis was performed at the cooperating BSs and the cooperating RNs for the objective of maximizing the rate of the cell-edge UEs.

CONTENTS

ILLUSTRATIONS

TABLES

LIST OF ABBREVIATIONS

LTE	Long Term Evolution cellular communication system
LTE-A	LTE-Advanced
CoMP	Coordinated Multipoint
CS	Coordinated Scheduling
CB	Coordinated Beam-Forming
JP	Joint Processing
UEs	User Equipment
BS	Base Stations
RNs	Relay Nodes
AF	Amplify and Forward
DF	Decode and Forward
EF	Estimate and Forward
IUI	Inter-User Interference
SINR	Signal to Interference plus Noise Ratio
CQI	Channel Quality Indicator
SVD	Singular Value Decomposition
QRD	QR-Decomposition
SQRD	Sorted- QR-Decomposition
RB	Resource Block
ZF	Zero Forcing
E-RSS	Exclusive RN sharing system
F-RSS	Fully RN sharing system
MRC	Maximum Ratio Combining
CSIT	Channel State Information at the Transmitter side
CrX2	Cooperative relay X2
MU-MIMO	Multi-User MIMO
SIC	Successive Interference Cancelation
AWGN	Additive White Gaussian Noise
BER	Bit Error Rate

CHAPTER I

INTRODUCTION

A. Motivation

The Internet participants nowadays are growing very fast and they are expected to reach 5 billion mobile broadband users worldwide by 2016 [1]. To meet this increasing demand, the Long Term Evolution cellular communication system (LTE) is being evolved in multiple aspects. Thus, the radio capabilities in LTE release 10 have changed considerably, leading to a significant improvement in the achievable data rates [2], where LTE-Advanced (LTE-A) is supposed to offer 1Gbps data rates in the downlink and 500Mbps in the uplink, partly enabled through aggregating LTE carriers to result in bandwidths of up to 100 MHz [5]. In my thesis the focus is on two main physical layer techniques that contribute to the realization of LTE-A, which are coordinated multipoint (CoMP) and relays, both of which will help in improving the cell edge throughput.

CoMP provides several benefits, including mitigating inter cell interference that affects the cell edge users, therefore leading to higher average data rates, as well as increasing the cell edge throughput [3]. Basically, two main schemes are used in CoMP transmission, 1) coordinated Scheduling and/or Beam-Forming (CS/CB), and 2) Joint Processing (JP) [3]. In JP-CoMP the data to be delivered to a UE is found at all or some Base Stations (BSs) in the cooperating set for simultaneous transmission, which results in improved received signal quality and throughput [4]. In CS/CB the data delivered to a UE originates from one BS in the CoMP coordinating set, whereas the user scheduling and beamforming decisions are made after the cooperation between BSs in the cooperating set [4].

Relay Nodes (RNs) in LTE-A are also deployed to increase the cell coverage and capacity [5] since they effectively decrease the distance between the BS and the UE. The RN is attached to the BS wirelessly through the Un interface and uses the same radio resources as a mobile UE, which in return is connected to the RN through the Uu interface [5]. The RNs can be of different types: Amplify and Forward (AF), Decode and Forward (DF), and Estimate and Forward (EF) [5]. The typical position of the RNs is about $2/3^{rd}$ of the cell radius [6], but an analysis on the DF-RN location in [7] shows that the optimum location is at 0.52 of the cell radius.

B. Objective

In the literature, JP-CoMP is designed based on three cooperating BSs that use precoding vectors to eliminate inter-user interference (IUI) [9][10][14][16]. In contrast to this design, I propose a new scheme where only two BSs need to cooperate. To eliminate the IUI, the design includes the RNs near the cell edge in the transmission scheme so that there is no need for a third BS. Moreover, the existing systems that combine CoMP and relaying together such as [5], [8], and [22] use one RN at the intersection of the cooperating set. My design is different than those in the literature since it exploits already deployed RNs in the cell coverage area.

C. Contributions

The contributions of my work are as follows:

- ✓ Exploiting already-deployed RNs in the cell to participate in JP-CoMP along with the BSs to enhance the system throughput and at the same time extend its capacity.
- ✓ Integrating sorted QR decomposition (SQRD) in the design for further performance improvement, and validating its superiority over other precoding techniques.
- ✓ Identifying the optimal RN locations in the involved cells.

✓ Testing the system's performance with imperfect channel conditions, and proving the resiliency of the design to error-prone channels.

✓ Presenting performance results that illustrate gains in terms of Signal to Interference plus noise Ratio (SINR) and capacity.

Hence, the outcome of the new design is twofold.

✓ Freed BSs, which allows the network to serve more users. Indeed, the reduction of the number of BSs in a cooperating cluster is preferred from a designer point of view, since the capacity will be increased in a specific coverage area [20]. Moreover, this reduction will lead to power reduction (Cooling system, RF amplifiers, etc.), and to a more energy efficient system [17].

✓ The data rates of the cell edge UEs will be higher than using CoMP or relaying separately, as we shall show in the experimental results. Indeed, and as was stated in [5], the combined solution improves the signal strength through relaying capabilities, while CoMP will be employed to cancel the inter-cell interference.

In the rest of this thesis Report, Chapter II represents the related work. Chapter III describe the proposed system and the precoding vector design, respectively. Chapter IV derives the optimal RN locations in the participating cells, while chapter V shows the power optimization problem formulation of the system design. Finally, Section VI concludes my thesis.

CHAPTER II

RELATED WORK

This section includes a general overview on how JP-CoMP can be implemented and its limitations that can be solved by introducing RNs in the cooperating cells. Next, the existing systems that combine CoMP and relaying together will be presented.

A. JP-CoMP for mitigating inter-cell interference

A JP-CoMP design that was proposed in [10] is based on three cooperating BSs that use precoding vectors to eliminate inter-user interference. The design consists of a cluster of three BSs, where UE1 and UE2 are in the overlap region of the cells of BS1 and BS2, whereas UE3 is near the cell center of BS3. The cell edge users UE1 and UE2 are served through the coordination of BS1, BS2 and BS3 to improve their signals, as well as to mitigate inter-user interference. The cell center user UE3 is only served by BS3, which is the one responsible for removing the interference at the cell edge users, through specific precoding vectors. Thus, BS3 combines the symbols intended to UE1 and UE2 by generating a network coded signal. Figure 2.1 shows the JP-CoMP system design used in [10] to serve the cell-edge UEs.
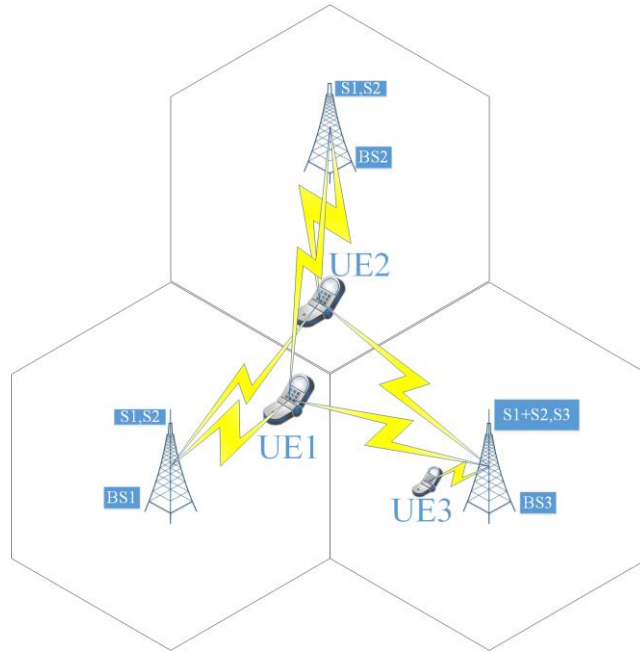
Figure 2.1: Three cells applying JP-CoMP

The proposed system in [12] uses JP-CoMP to suppress inter-cell interference. The process of the algorithm in [12] is as follows:

1. Generate the coordinating cluster

2. Selecting the users that must undergo coordination which are the cell edge users. The cell edge users and the cell center users are identified in [12] through comparing the path loss difference with a certain threshold.

3. Resource scheduling is done as follows:

   a) Every BS select a group of users from the total users in the cell to enter frequency domain scheduling based on the channel quality indicator (CQI) conveyed by the UE to the BS.

   b) Each BS have to compute for every resource block (RB) the priority parameter of the user. The priority parameter in [12] is the maximum transmission rate of a specific user at a specific time (t) divided by the average transfer rate of the same user before t.

c) Then every RB will be assigned two candidate users that correspond to the maximum priority users. In this way every RB in each BS in the cluster will have a candidate user list.

d) Finally the optimal users will be chosen in such a way for maximizing capacity. For a certain RB the first user that will be scheduled corresponds to the one with highest priority in the first candidate user list, then the second scheduled user will be the one that has the best channel orthogonality with user 1 chosen from candidate list 2, then the third scheduled user will be the one that has the best channel orhogonality with user 1 and user 2 chosen from candidate list 3, and the algorithm goes on until all users are scheduled.

4. The joint precoding algorithm is responsible to stop the IUI in the BS. In [12] the proposed algorithm uses the joint precoding algorithm that is based on block diagonalization.

5. User reception: In this step the SINR, CQI are calculated as well as reporting CQI and the precoding matrix index.

B. JP-CoMP Limitations

In JP-CoMP one of the cooperating BSs will receive the downlink data and transport them to the cooperating BSs through the X2 interface. Then all the cooperating BSs will transmit the data simultaneously to the cell edge UE in order to enhance its received signal [23]. A problem with JP concerns the sensitivity of data transmission due to the UE's mobility, as well as timing mismatches [3]. A solution for this problem is to use fixed RNs since RNs have known location and higher heights (6m) than the mobile UEs (1.6m), which leads to a decrease in the time variance. However, deploying many RNs in fixed locations is costly and may be infeasible, which makes it for certain schemes that are based on JP-CoMP, such as [6], challenging from a practicality standpoint . As shown in [6] JP-CoMP faces two

main challenges: precise channel estimation and high feedback overhead; therefore it is shown in [6] that the link between the BS and the RN can provide better CQI accuracy and less feedback overhead. For the above reasons I selected a design that achieves JP-CoMP through relaying.

C. JP-CoMP and Relaying systems

The system model in [5] installs one RN at the middle of every cluster where the three cells meet. The RN is full duplex and uses the Amplify and Forward technique. It receives the signals coming from the BSs in the cluster, which are intended to several UEs, it then amplifies and forwards them. The UE then adds all the signals coming from the cooperative BSs and the RN. When the system contains several users, the transmitted symbols vector will be produced through a weighted linear combination of the data symbols found in the vector d=[$d1$ $d2$ … dk]^T, where d_k is the symbol of the kth UE. In this case the UE will get undesired symbols, thus requiring the BS to apply the zero forcing (ZF) technique to design the precoding vectors to eliminate such symbols. In this respect, to be able to apply ZF, the BS must have knowledge of the CQI.

In [8] two system models were introduced in which the RN is placed at the intersection of two neighboring BSs where UE1 is at the cell edge of BS1 and UE2 is at the cell edge of BS2. These models are the exclusive RN sharing system (E-RSS) and the fully RN sharing system (F-RSS) [8]. In E-RSS, the RN is used by one of the two cooperating BSs to transmit the data at each transmission slot. The central control unit selects in an opportunistic way the BS that will use the RN to serve its cell edge UE in order to maximize the sum rate of the UE, thus leading to unfairness between the cell edge users. In the latter system, both BSs will transmit simultaneously the symbols intended for their cell edge UEs. If the control unit chooses BS1 to use the RN to serve its cell edge user UE1 then BS2 will serve its cell edge user UE2 through direct transmission. Thus, the RN will suffer from

interference due to BS2 transmission so precoding vectors are designed at the BSs to eliminate the interfering symbol at the RN. Then at a second time slot the RN will retransmit the decoded data received by BS1 to UE1, which will in return use maximum ratio combining (MRC) to combine both signals. On the other hand, in F-RSS the RN is used by the two cooperating BSs for data transmission. In F-RSS BS1 and BS2 transmit their symbol sequentially at different time slots therefore the signals will be received at the RN and the cell edge UE with no interference but this consequences in capacity loss. Then at phase 2, the symbols received at the RN will be precoded and transmitted simultaneously with precoded data from the BSs to the cell edge UE, thus useful signals are added up and interfering symbols will be eliminated. ZF is also used to design the precoding vectors. Finally, since the RN uses DF, then the achievable rate at the RN (R_{RN}) should meet the below condition so it can decode the transmitted signal.

$$R_{RN} \leq \log_2(1 + \gamma_{RN}) \qquad\qquad (1)$$

where γ_{RN} is the received SNR at the RN.

In [21] the BSs in the coordination set are supported by a specific number of RNs that will deliver the messages to K UEs where every UE is attached to one RN. The cooperating BSs will transmit to all RNs at predefined time $\alpha 1$ while applying Block diagonalization – zero forcing precoding [21]. Then each RN will transmit the data intended for its associated UE on a predefined time $\alpha 2 = 1 - \alpha 1$, meaning that interference could occur due to simultaneous RNs transmissions and no RN coordination [21]. Since no channel state information at the transmitter side (CSIT) is available at the RN, then the achievable rate of the link between the RN and the UE is affected by interference, and follows the conventional MIMO capacity expression [21] that is affected by the interference produced by the transmissions of neighboring RNs. The proposed system in [21] tried to improve the spectral efficiency degradation due to half-duplex relaying through BS coordination and through

8

optimizing the radio resources that are subject to the convex performance criteria, which is limited by the power constraint and the modulation and coding scheme of each BS, as well as the transmission rate at the RN-UE link.

The approach in [24] uses a relay system that is based on OFDM to serve cell edge UEs, where cooperative BSs transmit the data simultaneously to the RN. Also, a co-phasing power allocation scheme was developed that aims to decrease the phase difference between the signal replicas on every sub-carrier received at the RN by each cooperative BS. A co-phasing "waterfilling" power allocation algorithm was also developed in [24] to maximize the attainable end-to-end rate.

CHAPTER III

SYSTEM DESIGN

A. System Setup

Our design considers two cooperating BSs where several RNs are assumed to be already deployed in every cell (illustrated in Figure 3.1). Moreover, our design implements a MIMO system where the BSs, RNs, and the UEs are equipped with multiple antennas and using a JP-CoMP transmission scheme due to its benefits. Since no CSIT is available at the RN, then the achievable rate of the link between the RN and the UE is affected by interference, and follows the conventional MIMO capacity expression [21] that is affected by the interference produced by the transmissions of neighboring RNs in the cell as stated above. The proposed design comprises operations that are grouped into two phases. In Phase 1, the cooperating BSs use JP-CoMP to send the same downlink data of their cell edge users to the RNs (one in each cell) that have the minimum distance to the cell edge UE, or to the one that has the best CQI with that UE. For the second criteria to be used, the RN must periodically send the CQI of cell edge users in its range to its serving BS and we assume that the RN is in Line of Sight with the BS. Then in phase 2, the chosen RNs in the cooperating set must communicate together to configure the proper precoding vectors responsible for eliminating the IUI due to the second transmission. The RNs cooperate through the cooperative relay X2 interface (crX2) [13] for signaling information exchange. Finally, the received signals from both phases will be combined using MRC at the UE.
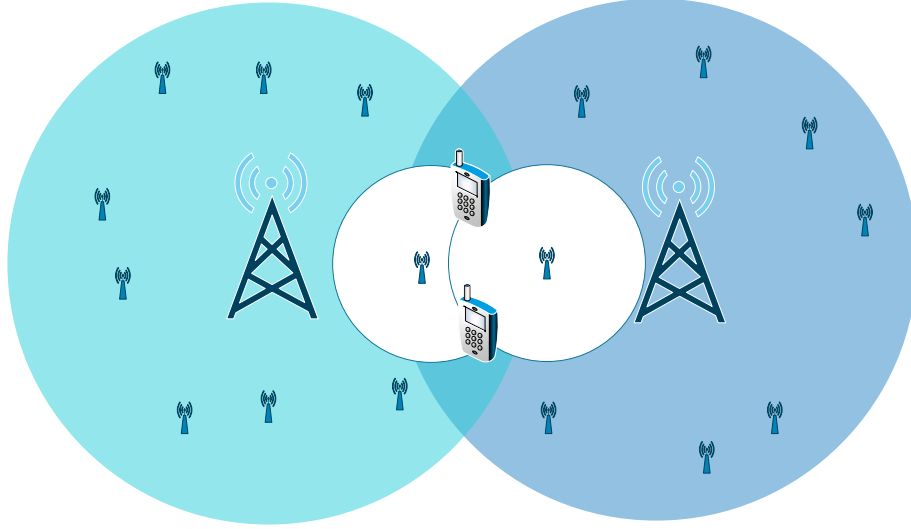
Figure 3.1: Overview of our proposed system design

Figure 3.2 shows the signals of both transmissions, where the solid lines represent the useful signal intended for the RN or for the cell edge UE, while the dashed lines show the interfering signals. The lines labeled (1) show the signals transmitted in the first time slot, while those labeled (2) show the signals transmitted in the second time slot. We consider a Multi- User MIMO (MU-MIMO) downlink system, where l cooperating BSs, each equipped with M_T transmit antennas, and K UEs equipped with M_{Ri} receive antennas for i=1, 2, …, K, and let $\mathbf{X} \in C^{lM_T \times KM_{Ri}}$ be the signal matrix to be transmitted to the cell-edge UEs. Then, if we denote the MIMO channel matrix between the cooperative BSs and the cell edge UE$_i$ as $\boldsymbol{H}_i \in C^{M_{Ri} \times lM_T}$, then the system's channel matrix is

$$\boldsymbol{H} = [H_1^T\ H_2^T\ ...\ H_K^T\ ]^T \qquad (2)$$

The received signal at the cell edge UE$_i$ is thus $\boldsymbol{y}_i \in C^{M_{Ri} \times 1}$

$$\mathbf{y} = \mathbf{HX} + \mathbf{n} \qquad (3)$$

where, $\mathbf{y} = [y_1^T, ..., y_K^T]^T$ and $\boldsymbol{n} = [n_1^T, ..., n_K^T]^T$ is the additive white Gaussian noise. The $(n,m)^{\text{th}}$ element (for $n = 1, ... , M_{Ri}$ and $m = 1, ... , l\ M_T$) in the channel matrix between cooperating BSs and the ith cell edge UE is as follows:

11

$$H_i(n, m) = \alpha_i^{n,m} \sqrt{\beta_i A(\theta_i^m) \left(\frac{d_l}{d_0}\right)^{-\gamma}} \qquad (4)$$

where $\alpha_i^{n,m}$ corresponds to the fast Rayleigh fading channel between the mth transmit antenna of the cooperating BSs and the nth receive antenna of the ith cell edge UE, β_i is the log-normal shadowing of the channel between the cooperating BSs and the ith cell edge UE, $A(\theta_i^m)$ represents the antenna gain of the mth transmit antenna at the cooperating BSs, d_l represents the distance from the lth cooperating BSs to the cell edge UE, d_0 corresponds to the reference distance from the center of the cell to the vertex of the cell, and γ corresponds to the pathloss exponent. Similarly, the channel between the BS and the RN from one side and between the RN and the UE from the other side is defined as in (4).

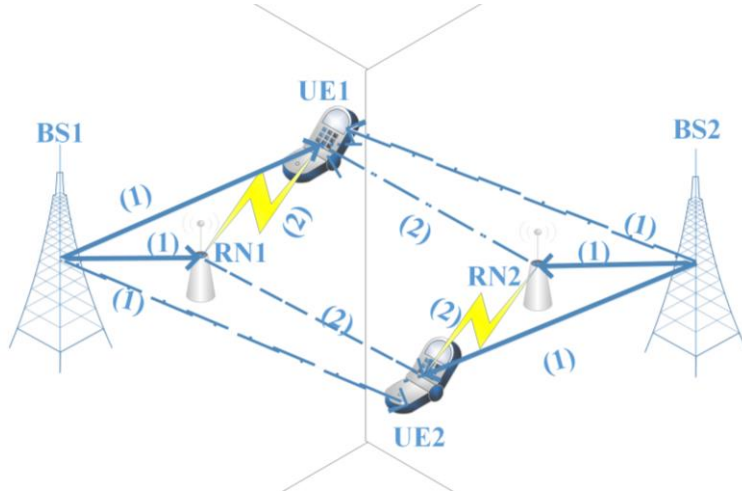

Figure 3.2: Useful and interfering signal in our system design

Knowing the channel matrix at the BSs and the RNs, the problem then boils down to finding the precoding vectors that remove the IUI. In our scheme, they are designed by applying Singular value decomposition (SVD), QR-Decomposition (QRD), and sorted QRD (SQRD) on the channel matrix $\boldsymbol{H}$.

B. Precoding Vector Design

In this section I will explore three techniques for precoding vector design, namely SVD, QRD, and SQRD. Later, I will demonstrate the superiority of the SQRD scheme, as expected.

1. Singular value decomposition (SVD)

For SVD [11], we consider $\boldsymbol{F}_i$ to be a diagonal matrix having the average signal power attained at the ith UE from the jth transmit antenna, where $\boldsymbol{F}_i \in C^{M_{R_i} \times lM_T}$

$$\boldsymbol{F}_i = diag\{\sqrt{P_{i,1}} \ \sqrt{P_{i,2}} \ \cdots \ \sqrt{P_{i,M_{R_i} \times lM_T}}\} \tag{5}$$

The term P_{ki} is the received signal power at the ith UE from the kth BS, determined by

$$P_{ki} = P_{tk} \times PL_{i,k} \times S_{i,k} \tag{6}$$

where P_{tk} is the transmit power by the kth BS, $PL_{i,k}$ is the pathloss, and $S_{i,k}$ is the shadowing between the kth BS and the ith UE. Therefore, the channel matrix between the cooperative BSs and the cell edge UEs can be seen as follows:

$$\boldsymbol{G} = [G_1 \ G_2 \cdots G_K]^T \tag{7}$$
$$= [(H_1F_1)^T \ (H_2F_2)^T \ \cdots \ (H_KF_K)^T]^T$$

If we let $\mathbf{x}_i$ be the data intended for the ith UE, then the transmitted matrix **X** by the cooperating BSs for all users could be written as: $\mathbf{X} = [\mathrm{x}_1^T \ \mathrm{x}_2^T \cdots \mathrm{x}_K^T]^T$ and the precoding matrix is $\boldsymbol{W} = [w_1 \ w_2 \cdots w_K]$ where w_i is the precoding vector for the ith UE created by the cooperating BSs.

Now, the objective is to find the precoding matrix designed to eliminate IUI. To do so, the received signal at the ith cell edge UE could be written as:

$$y_i = G_iw_i\mathrm{x}_i + \sum_{j \neq i}^{K} G_iw_j\mathrm{x}_j \ + n_i \tag{8}$$

The first term of the right hand side in (7) represents the useful signal while the second is the interfering signal. To eliminate the latter component, the following condition should be met:

13

$$G_i w_j = 0 \quad for \; \forall j \neq i$$

The interfering channel matrix $\overline{G}_i$ for every user is defined as

$$\overline{G}_i = [(G_1)^T \cdots (G_{i-1})^T (G_{i+1})^T (G_K)^T]^T \qquad (9)$$

To eliminate the interference at the ith UE, w_i must be in the null space of $\overline{G}_i$. This means the following should be satisfied:

$$l \times M_T \geq K \times M_R \qquad (10)$$

In this section, the precoding vectors are designed according to the SVD of $\overline{G}_i$. This yields the following:

$$\overline{G}_i = \overline{U}_i \left(\begin{matrix} \overline{\sum} i & 0 \\ 0 & 0 \end{matrix} \right) [\overline{V}_i^{(1)}, \overline{V}_i^{(0)}]^H \qquad (11)$$

where $\overline{\sum} i$ is a diagonal matrix that contains the singular values of $\overline{G}_i$, $\overline{V}_i^{(1)}$ and $\overline{V}_i^{(0)}$ are the singular vectors, and H represents the Hermitian transpose. The singular vector $\overline{V}_i^{(0)}$ corresponds to the null singular value of $\overline{G}_i$ and therefore it builds an orthogonal basis for the null space of $\overline{G}_i$. The independent data streams that can be delivered to the ith UE must be smaller than the columns of $\overline{V}_i^{(0)}$[12]. Therefore, we choose t_i columns from the right of $\overline{V}_i^{(0)}$ to be the block diagonalization precoding matrix of user i, and denote it as $\overline{\overline{V}}_i^{(0)}$. The SVD of the effective channel matrix $G_i \overline{\overline{V}}_i^{(0)}$ is as follows:

$$G_i \overline{\overline{V}}_i^{(0)} = U_i \sum_i V_i^H \qquad (12)$$

The precoding matrix W will then be written as:

$$W = [w_1 \; w_2 \cdots w_K]$$

$$= \left[\frac{1}{\sqrt{t_1}} \overline{\overline{V}}_1^{(0)} V_1 \cdots \frac{1}{\sqrt{t_2}} \overline{\overline{V}}_2^{(0)} V_2 \frac{1}{\sqrt{t_K}} \overline{\overline{V}}_K^{(0)} V_K \right] \qquad (13)$$

where t_i is the independent data stream to be sent with the same power to every UE. In the first transmission phase, the RNs will be receiving the symbols intended for the edge UEs. I adopted ZF equalizer for decoding purposes. In the second phase, the same procedure will be applied by the RNs. That is, SVD will be used to design the joint precoding vectors. Finally, the UE will adopt MRC to detect the signals.

2. QR decomposition (QRD)

In a non-CoMP scenario, SVD is used to design the optimum precoding vectors as seen in [18]. However, in CoMP the channel matrices of the cooperating BSs must be in-phase to improve the equivalent precoded channel. Hence, to improve performance, I propose to design the precoding vector using a pre-phase adjustment based on QRD [18]. The QRD on $\boldsymbol{H}_i$ consists of writing the channel matrix as follows:

$$\boldsymbol{H}_i = R_i \boldsymbol{Q}_i^H \tag{14}$$

where $\boldsymbol{Q}_i$ is a unitary or semi-unitary matrix and $\boldsymbol{R}_i$ is the lower triangular matrix, shown below:

$$\boldsymbol{R}_i = \begin{bmatrix} r_{1,1}^{(i)} & 0 & \cdots & 0 \\ r_{2,1}^{(i)} & r_{2,2}^{(i)} & \cdots & 0 \\ \vdots & \vdots & \vdots & \vdots \\ r_{M_{R_i},1}^{(i)} & r_{M_{R_i},2}^{(i)} & \cdots & r_{M_{R_i},M_{R_i}}^{(i)} \end{bmatrix} \tag{15}$$

Then the diagonal matrix $\boldsymbol{F}_i$ for pre-phase regulation of $\boldsymbol{R}_i$ is:

$$\boldsymbol{F}_i = \begin{bmatrix} \dfrac{(r_{1,1}^{(i)})^*}{|r_{1,1}^{(i)}|} & 0 & \cdots & 0 \\ 0 & \dfrac{(r_{2,2}^{(i)})^*}{|r_{2,2}^{(i)}|} & \cdots & 0 \\ \vdots & \vdots & \ddots & \vdots \\ 0 & 0 & \cdots & \dfrac{(r_{k,k}^{(i)})^*}{|r_{k,k}^{(i)}|} \end{bmatrix} \tag{16}$$

15

The precoding vector at every BS, denoted by $\mathbf{w}_i \epsilon C^{M_T \times k}$ where k is the transmit rank of every UE, is given by:

$$\mathbf{w}_i = Q_i(:,1:k)F_i \qquad (17)$$

Then the precoded channel matrix $H_i w_i$ is as follows:

$$
H_i w_i
$$

$$
= \begin{bmatrix}
\sum_{i=1}^{l}\left|r_{1,1}^{(i)}\right| & \cdots & 0 \\
\vdots & \ddots & \vdots \\
\sum_{i=1}^{l} r_{k,1}^{(i)}\frac{(r_{1,1}^{(i)})^*}{\left|r_{1,1}^{(i)}\right|} & \cdots & \left|r_{k,k}^{(i)}\right| \\
\vdots & \ddots & \vdots \\
\sum_{i=1}^{l} r_{M_{R_i},1}^{(i)}\frac{(r_{1,1}^{(i)})^*}{\left|r_{1,1}^{(i)}\right|} & \cdots & \sum_{i=1}^{l} r_{M_{R_i},k}^{(i)}\frac{(r_{k,k}^{(i)})^*}{\left|r_{k,k}^{(i)}\right|}
\end{bmatrix} \qquad (18)
$$

Finally, to detect the useful signal, a successive interference cancelation (SIC) receiver must be used along with MRC for the signal obtained through the two phases.

3. Sorted QR decomposition (SQRD)

The main drawback of QRD is that the energy spread along the diagonal terms is not balanced [19]. Therefore, SQRD is used to enhance the magnitude spread of the diagonal elements in the triangular matrix [19] of the decomposed channel matrix. As a result, the spatial pipes that experience deep fading will be minimized. We apply SQRD on the channel matrix $\mathbf{H}$ through a permutation matrix so that there is reduced error propagation in the conventional QR decomposition, as follows

$$\mathbf{H}^{\mathbf{H}}\boldsymbol{\pi}^{\mathbf{H}} = \mathbf{Q}\mathbf{R}^{\mathbf{H}} \ or \ \mathbf{H} = \boldsymbol{\pi}^{\mathbf{H}}\mathbf{R}\mathbf{Q}^{\mathbf{H}} \qquad (19)$$

where $\boldsymbol{\pi}$ is the permutation matrix. Then, I define the permuted symbol matrix $\mathbf{X}_{\boldsymbol{\pi}} = \boldsymbol{\pi}\mathbf{X} = [x_{\pi,1} \dots x_{\pi,KM_{R_i} \times lM_T}]^T$ that will be transmitted, and which represents user re-ordering in QR decomposition. Consider the diagonal matrix $\mathbf{F} = diag([f_1, \dots, f_{KM_{R_i} \times lM_T}])$ used for power

allocation on the decomposed spatial pipes of the channel matrix. Then, the element $\tilde{x}_{\pi,k}$ in the vector $\boldsymbol{X}_{\boldsymbol{\pi}}$ is calculated as follows

$$\tilde{x}_{\pi,k} = mod\left(x_{\pi,k} - \sum_{j=1}^{K-1} \frac{r_{k,j}f_j}{r_{k,k}f_k} \tilde{x}_{\pi,j} \right), k \qquad (20)$$

$$= 1,2,\dots,K$$

Therefore, $\boldsymbol{W}$ is reduced to a diagonal matrix where the ith diagonal element is $w_i = (r_{i,i}f_i)^{-1}$. Hence, at every receiving antenna the signal will be detected as:

$$\hat{x}_i = mod(w_i y_i) \qquad (21)$$

C. System Simulation Under Different Decompositions

The simulation setup considers two cooperating BSs each equipped with two antennas, and two RNs installed at $2/3^{rd}$ the radius away from the cell center and also each equipped with two antennas. The RNs operate in half-duplex DF mode, and the modulation used is BPSK. The system contains two cell-edge UEs each equipped with two antennas, where UE1 is at the cell edge of BS1 and UE2 is on the side of BS2. At every receiver, assume that the noise is additive white Gaussian (AWGN) with zero mean and variance σ^2. Figure 3.3 shows how the Bit Error Rate (BER) of the system, when perfect channel estimation is considered, outperforms the BER performance of JP-CoMP in the literature. The results also show that the system experiences higher throughput when SQRD is used instead of QR and SVD.
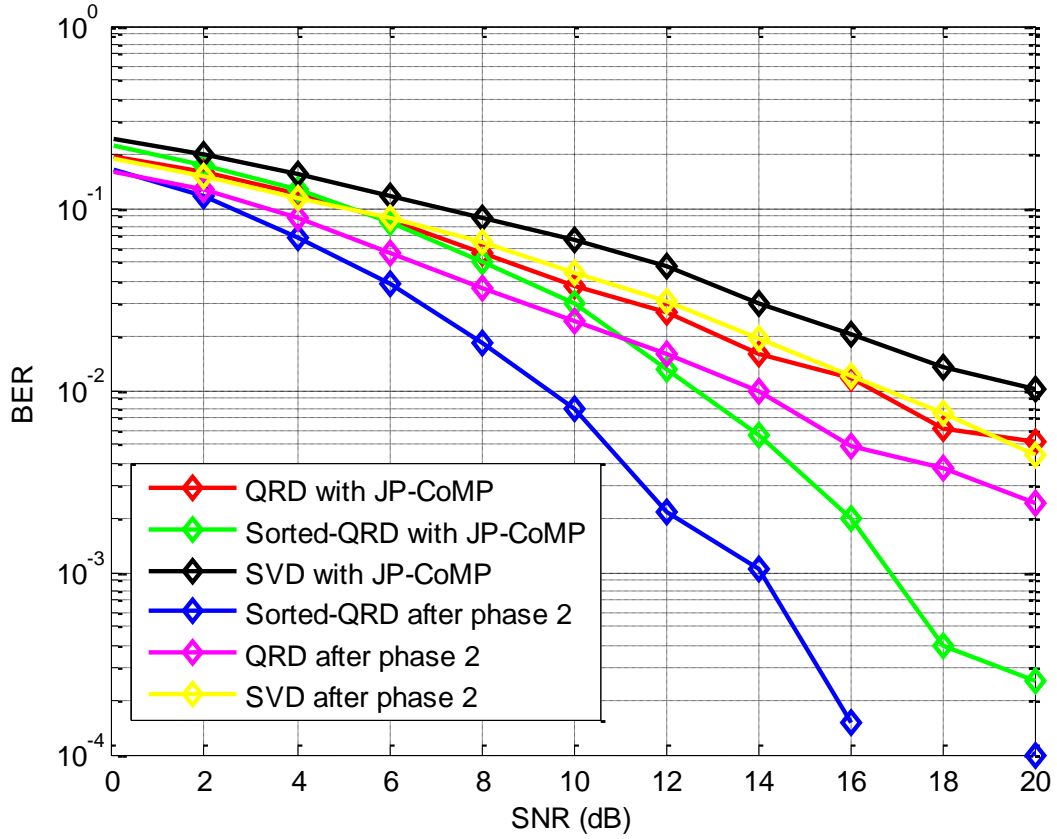
Figure 3.3: BER Performance of our system Design

Figure 3.4 shows the BER performance under real channel estimation with different estimation error variances and SQRD precoding scheme. The figure shows that an increase in the estimation error variance leads to degradation in the BER performance. Furthermore, it shows that the system is more robust to real channel estimation than conventional JP-CoMP, proposed in the literature. Figure 3.5 compares the SINR Cumulative Distributive Function (CDF) of the proposed JP-CoMP system and the conventional scheme (i.e. three cooperating BSs). This figure illustrates that my design outperforms those in the literature by about 4dB improvement. Figure 3.6 shows that the system provides about 2 bps/Hz improvement over the conventional JP-CoMP systems with three cooperating BSs.

18

Figure 3.4: BER performance due to channel estimation error

Figure 3.5: The CDF of the receive SINR at the UE
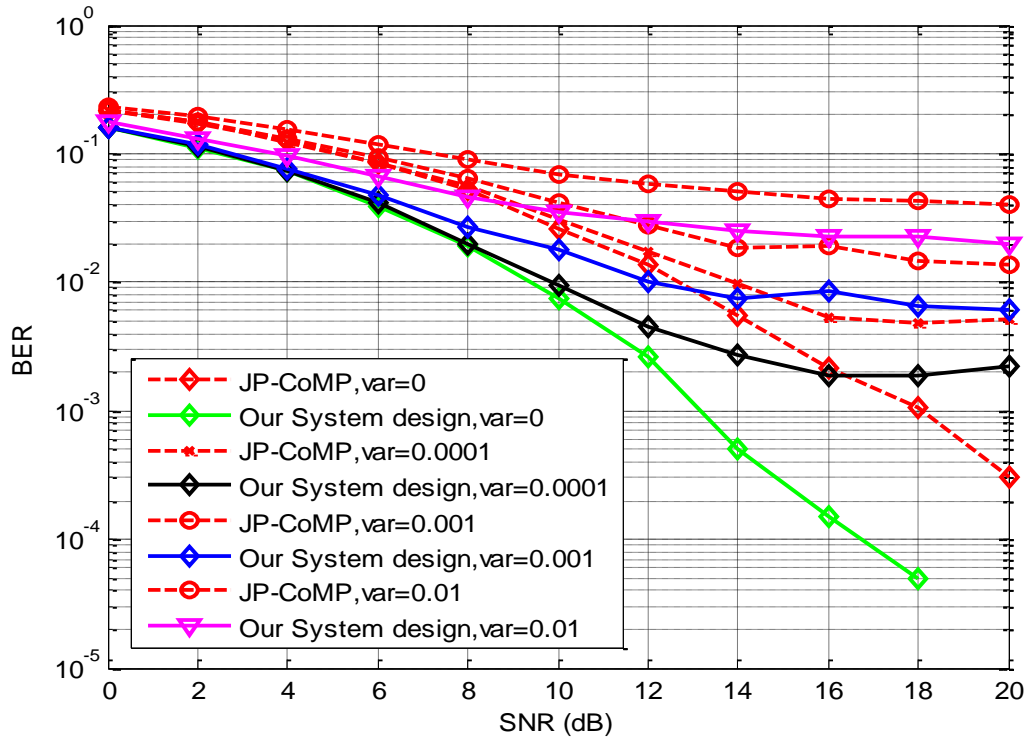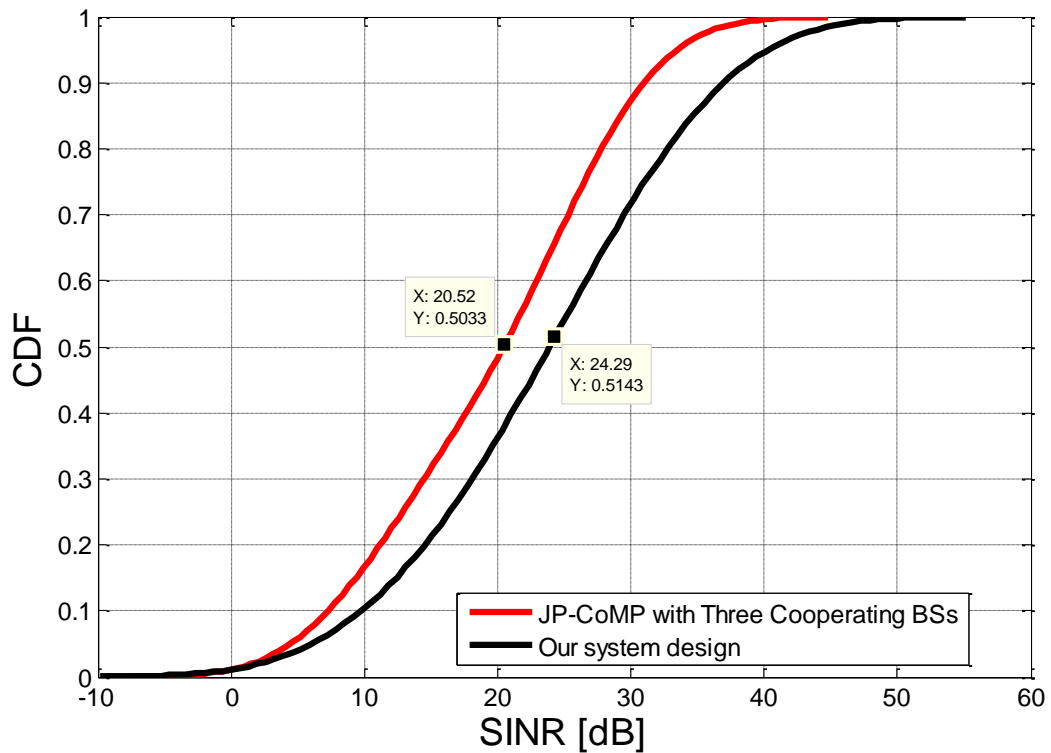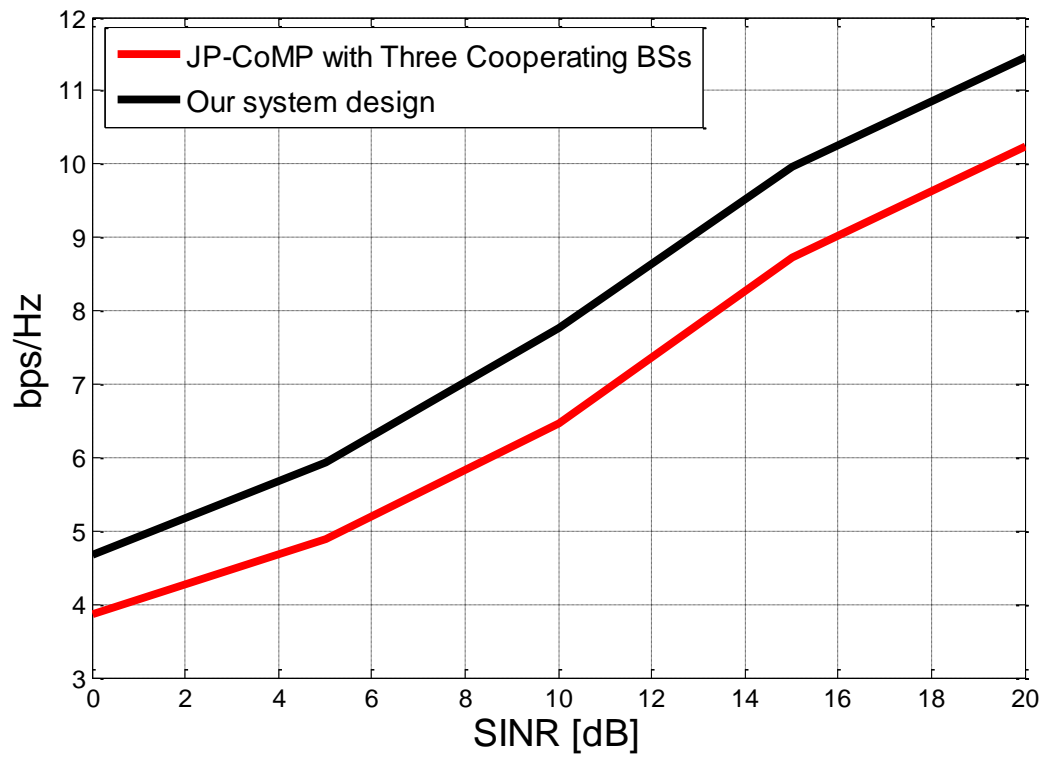
Figure 3.6: Capacity of our system design

CHAPTER IV

FINDING OPTIMAL RN LOCATION

In this section the optimal locations of the cooperating RNs are studied in order to accomplish the maximum data rate at the cell-edge UE. The coordinating BSs and the UE locations are known, as well as the transmission power at the BSs and the RNs. When the distance between the BS and the UE increases the received power decreases. Hence, the optimal location of the RN has to be on the line between the BS and the edge UE [7]. I assumed a fixed distance between every cooperating BS and the cell edge UE (shown in Figure 4.1). Then, we set the distance BS−RN as d_{BS-RN}, the distance BS−UE as d_{BS-UE}, the distance RN−UE as d_{RN-UE}. We also consider, $d_{BS-RN} = q d_{BS-UE}$ for $q \in (0,1)$, and $d_{RN-UE} = (1-q)d_{BS-UE}$. Assuming that the interference term is neglected due to the precoding vectors design at the cooperative BSs and RNs that are responsible for interference cancellation, then the SNR for each transmission phase at each receiving antenna of the UE is

$$SNR_{BS-UE,i} = \frac{\boldsymbol{P_{BS}} \left| \boldsymbol{H_{BS-UE,i}} \right|^2}{N_0} \tag{22}$$

$$SNR_{BS-RN} = \frac{\boldsymbol{P_{BS}} \left| \boldsymbol{H_{BS-RN}} \right|^2}{N_0} \tag{23}$$

$$SNR_{RN-UE,i} = \frac{\boldsymbol{P_{RN}} \left| \boldsymbol{H_{RN-UE,i}} \right|^2}{N_0} \tag{24}$$

where, $\boldsymbol{P_{BS}}$ is a 1×2 vector that contains the power of the two cooperating BSs while $\boldsymbol{P_{RN}}$ contains the power of the two cooperating RNs. $\boldsymbol{H_{BS-UE,i}}$, $\boldsymbol{H_{BS-RN}}$, and $\boldsymbol{H_{RN-UE,i}}$ are 2×1 vectors of the channel between the cooperative BSs and the ith edge UE, channel between

cooperative BSs and cooperative RNs, and channel between cooperative RNs and the ith cell edge UE, respectively. Finally, N_0 is the noise variance.
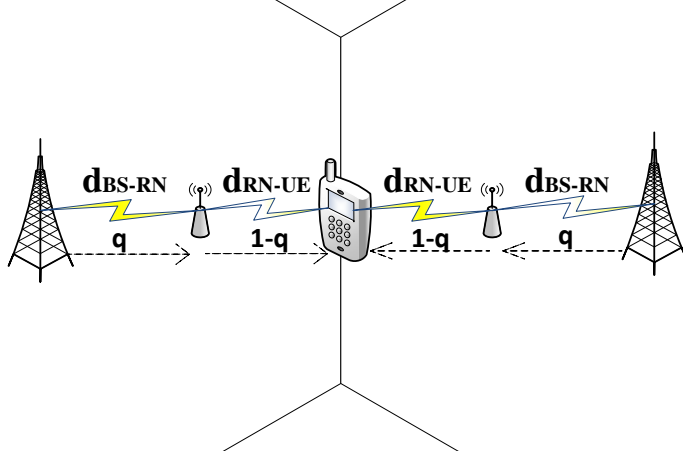
Figure 4.1: Optimizing RN location

For simplicity, we consider that the channel coefficient between any source i and destination j is a function of pathloss [7]:

$$\left|H_{i-j}\right|^2 = \left(d_{i-j}\right)^{-\gamma} \tag{25}$$

where d_{i-j} is the distance between the ith source and the jth destination and γ is a factor, typically $\gamma \in [2-5]$. The achievable rate at the edge UE when using DF-RN [15] is:

$$R_{UE,i}^{DF} = min\{R_{UE,i}^{DF}(1), R_{UE,i}^{DF}(2)\} \tag{26}$$

$$R_{UE,i}^{DF}(1) = \frac{1}{2}\log_2(1 + SNR_{BS-RN}) \tag{27}$$

$$R_{UE,i}^{DF}(2) = \frac{1}{2}\log_2\big(1 + SNR_{BS-UE,i} \tag{28}$$

$$+ SNR_{RN-UE,i}\big)$$

where $R_{UE,i}^{DF}(1)$ is the rate of the backhaul link between the cooperative BSs and the chosen RNs for cooperation. $R_{UE,i}^{DF}(2)$ is the overall rate of both the direct link when the cooperative BSs are transmitting to the UE in the first phase and the access link when the cooperative

RNs are transmitting to the cell edge UE in the second phase. $R_{UE,i}^{DF}$ is the overall rate of our system. Then,

$$SNR_{BS-UE,i} + SNR_{RN-UE,i}$$

$$= \frac{P_{BS}d_{BS-UE,i}^{-\gamma}}{No} + \frac{P_{RN}((1-q)d_{BS-UE,i})^{-\gamma}}{No} \qquad (29)$$

$$SNR_{BS-RN} = \frac{P_{BS}(qd_{BS-UE,i})^{-\gamma}}{No} \qquad (30)$$

The optimal distance of the relay node is thus the one that achieves the maximum rate at the edge UE, i.e., the one required to find the maximum value reached in Equation (26).

Figure 4.2 shows the achievable rate versus the RN location at the edge UE with the path loss coefficient γ set to 4. It is seen from the figure, and summarized in Table 4.1, that as the Power Ratio (PR) P_{RN}/P_{BS} increases the RN location should be closer to the BS.

Table 4.1 below shows the location of the RN that maximizes the achievable rate at the cell edge UE in our system design versus its location if one cell is taken into consideration.

Table 4.1. Optimum Location of RNs versus RN power variation

P_{RN}/P_{BS}	0.1	0.15	0.2	0.25	0.3	0.35	0.4
d_{BS-RN} CoMP	0.63	0.61	0.59	0.58	0.57	0.56	0.55
d_{BS-RN} (single cell)	0.6	0.58	0.56	0.55	0.54	0.53	0.52
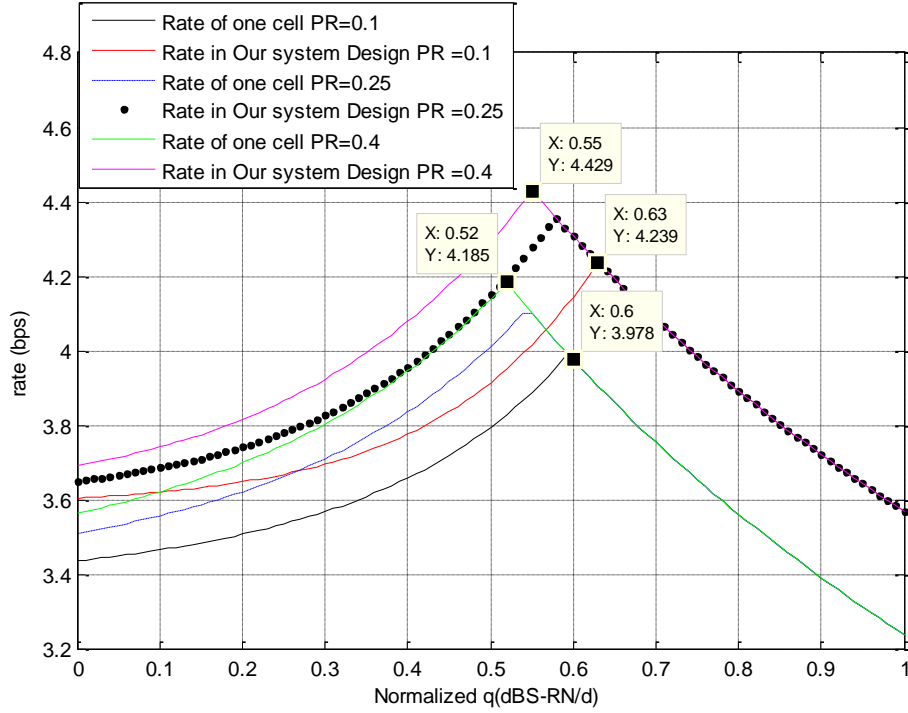
Figure 4.2: Rate achieved at cell edge UE for different RN power

Now, if we consider the real channel represented by equation 4 the SNR equations will

depend on $\alpha_i^{n,m}, \beta_i, and\ A(\theta_i^m)$ as seen below.

$$SNR_{BS-UE,i}$$

$$= \frac{P_{BS} \cdot (\alpha_{i,BS-UE}^{n,m})^2 \cdot \beta_{i,BS-UE} \cdot A(\theta_{i,BS-UE}^m) \cdot d_{BS-UE,i}^{-\gamma}}{No} \qquad (31)$$

$$SNR_{RN-UE,i} =$$

$$\frac{P_{RN} \cdot (\alpha_{i,RN-UE}^{n,m})^2 \cdot \beta_{i,RN-UE} \cdot A(\theta_{i,RN-UE}^m) \cdot ((1-q)d_{RN-UE,i})^{-\gamma}}{No} \qquad (32)$$

$$SNR_{BS-RN,i}$$

$$= \frac{P_{BS} \cdot (\alpha_{i,BS-RN}^{n,m})^2 \cdot \beta_{i,BS-RN} \cdot A(\theta_{i,BS-RN}^m) \cdot (qd_{BS-UE,i})^{-\gamma}}{No} \qquad (33)$$

When we take into consideration a Rayleigh fading channel the optimum location of the RN must be closer to the cell edge as seen in the figure below and summarized in table 4.2.
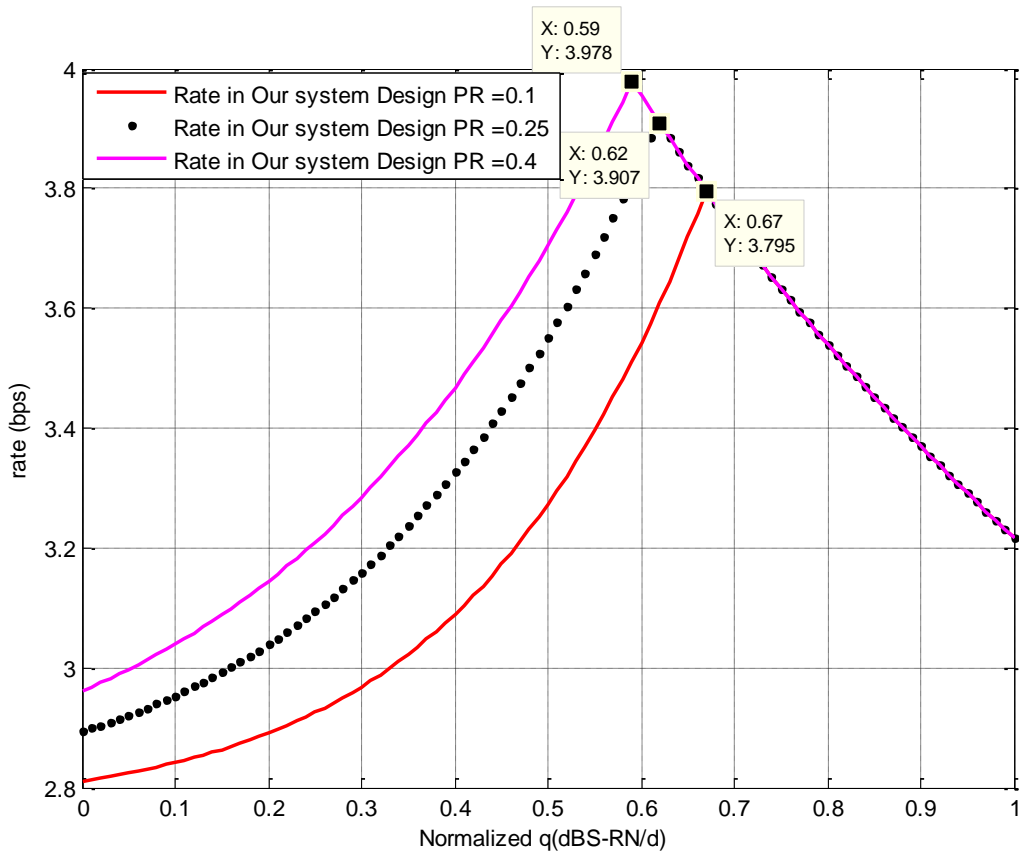
Figure 4.3: Rate achieved at cell edge UE under Rayleigh Fading channel

Table: 4.2 Optimum Location of RNs under Rayleigh Fading Channel

P_{RN}/P_{BS}	0.1	0.25	0.4
d_{BS-RN} CoMP (Pathloss model)	0.63	0.58	0.55
d_{BS-RN} CoMP with Rayleigh fading Channel	0.67	0.62	0.59

In a real case scenario the UE is not exactly at the cell edge and the RNs will not be exactly at the optimal locations for obtaining maximum rate. A real scenario is shown in the figure below.
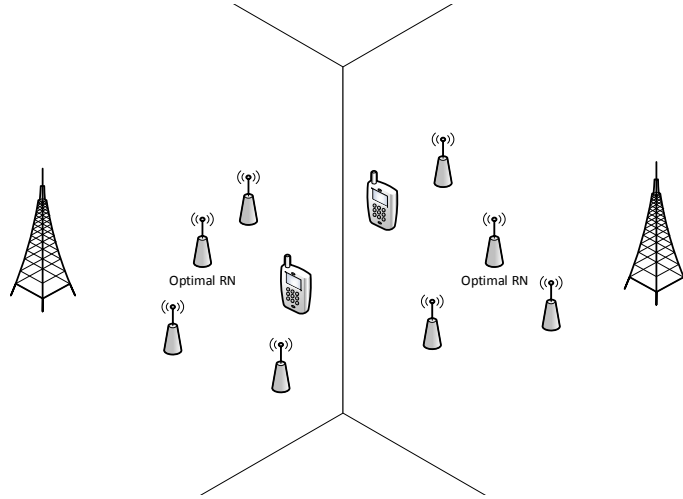
Figure 4.4: RNs and UEs under Real case scenario

In a real case scenario a cell – edge UE is considered to be between 0.9 and 1 of the cell radius. Moreover, the RNs are not necessary always at the optimal location that we have derived before, since RNs are found randomly in the cell. In this case, I have simulated the overall rate of my system while choosing the RNs that are closest to the cell edge UEs to undergo coordination. Furthermore, I repeated the simulation while choosing the RNs that are the closest to the optimal RN location to undergo coordination. The CDF of the overall rate at the cell-edge UE is seen in the figure 4.5 when the RN density in the cell is 4.
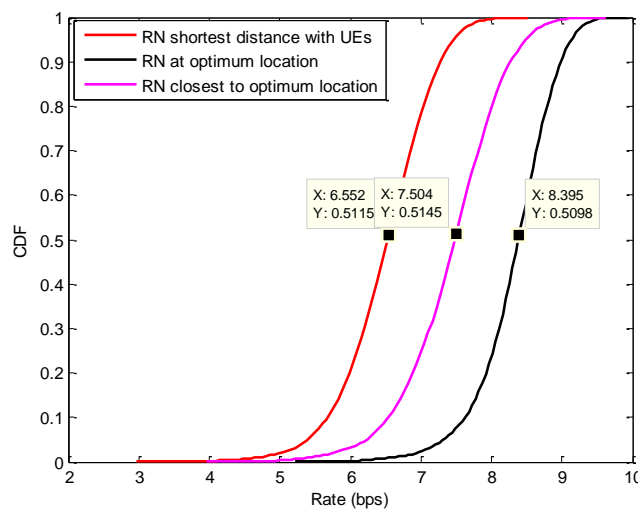
Figure 4.5: CDF of the overall Rate at the cell - edge UE with RN density =4
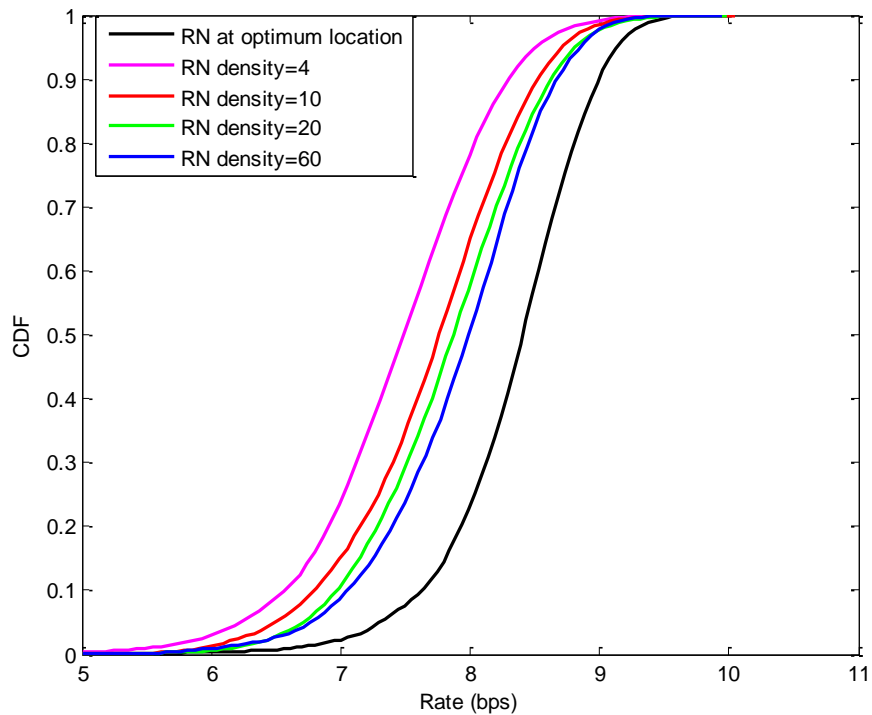
Figure 4.6: CDF of the overall Rate at the cell - edge UE while varying RN density

Figure 4.5 shows that if we choose the RN with closest distance to the cell edge UE we get about 1.8bps degradation in the rate in comparison with choosing the RN at optimum location. If we choose the RN with closest distance to the optimum location we get about 0.8 bps degradation in the rate in comparison with choosing always the RNs at optimum location to serve the cell-edge UEs as seen in figure 4.5. Figure 4.6 shows that as we increase the RN density in the cell (i:e from 4 to 60) the system performance of choosing the RN that is closest to the optimum location becomes very close to the system performance when we always choose the RNs at optimum locations.

CHAPTER V

OPTIMIZATION FORMULATION

A. Defining The Optimization Problem

In this section, the optimization problem formulation will depend on the SINR of each phase. The equations include the precoding vectors and the interference term that were ignored in the previous section. The interference term is taken into consideration since in practice the signals received at the UE are not well synchronized, therefore the interference term will not be zero. The system contains N RBs, which are assigned to serve one or more UEs. Consider, that the UEs that are scheduled at the nth RB correspond to the set $\mathcal{S}_n$. Now, the signal received at the ith UE over the nth RB due to the first transmission by the cooperating BSs is

$$y_{i,n} = h_{i,n} w_{i,n} \sqrt{p_{BS,i,n}} x_{i,n} + \sum_{\substack{j=1 \\ j \neq i}}^{K} h_{i,n} w_{j,n} \sqrt{p_{BS,j,n}} x_{j,n} + \eta_{i,n} \tag{34}$$

where, $h_{i,n}$, $w_{i,n}$, and $\sqrt{p_{BS,i,n}}$ are the channel, precoder, and power vector when the signal is transmitted to the ith UE on the nth RB, respectively. Whereas, $w_{j,n}$ and $\sqrt{p_{BS,j,n}}$ are the precoder and power vector allocated to the jth UE on the nth RB, respectively.

Since the power allocation in our system is done according to the SINR metric, I will start by defining the SINR of every transmission. First, the $SINR_{BS-UE_{i,n}}$ is defined between the cooperative BSs and the ith UE on the nth RB after the transmission in phase 1

$$SINR_{BS-UE_{i,n}} = \frac{\|h_{i,n}w_{i,n}\|^2 p_{BS,i,n}}{\sum_{j \in \mathcal{S}_n, j \neq i} \|h_{i,n}w_{j,n}\|^2 p_{BS,j,n} + \sigma^2} \tag{35}$$

At phase 2, R cooperating RNs will help in the retransmission for the users in the set $\mathcal{S}_n$. The SINR between the cooperating BSs and the cooperating RN in the serving cell of the ith UE over the nth RB is

$$SINR_{BS-RN_{i,n}} = \frac{\|\overline{h_{i,n}}w_{i,n}\|^2 p_{BS,i,n}}{\sum_{j \in \mathcal{S}_n, j \neq i} \|\overline{h_{i,n}}w_{j,n}\|^2 p_{BS,j,n} + \sigma^2} \tag{36}$$

where, $\overline{h_{i,n}}$ is the channel matrix between the cooperating BSs and the cooperating RN in the serving cell of the ith UE.

Similarly, the SINR at the second phase when the cooperative RNs are transmitting to the ith cell edge UE over the nth RB is

$$SINR_{RN-UE_{i,n}} = \frac{\|h_{RN,i,n}w_{RN,i,n}\|^2 p_{RN,i,n}}{\sum_{j \in \mathcal{S}_n, j \neq i} \|h_{RN,i,n}w_{RN,j,n}\|^2 p_{RN,j,n} + \sigma^2} \tag{37}$$

where, $h_{RN,i,n}$ is the channel matrix between the cooperative RNs and the ith cell edge UE on the nth RB, $w_{RN,i,n}$ is the precoder of the RN for the ith UE on the nth RB, and $p_{RN,i,n}$ is the power allocated by the cooperating RNs for the ith UE on the nth RB.

Now, the rate of our system depends on SINR, and it becomes as follows

$$R_{UE,i,n}^{DF}(p_{BS,i,n}, p_{RN,i,n}) = min\{R_{UE,i,n}^{DF}(1), R_{UE,i,n}^{DF}(2)\} \tag{38}$$

$$R_{UE,i,n}^{DF}(1) = \frac{1}{2}\log_2\left(1 + SINR_{BS-RN_{i,n}}(p_{BS,i,n})\right) \tag{39}$$

$$R_{UE,i,n}^{DF}(2) = \frac{1}{2}\log_2\left(1 + SINR_{BS-UE_{i,n}}(p_{BS,i,n})\right. \tag{40}$$

$$\left. + SINR_{RN-UE_{i,n}}(p_{RN,i,n})\right)$$

Our power allocation algorithm is based on allocating power to every UE being served, based on two constraints the total power of the BS and the total power of the RN.

Now, we can define our optimization problem as follows

$$\underset{\forall p_{BS,i,n} \geq 0 \ \& \ p_{RN,i,n} \geq 0}{\text{maximize}} \sum_{i \in \mathcal{K}_m} R_{UE,i,n}^{DF}\left(p_{BS,i,n}, p_{RN,i,n}\right) \tag{41}$$

$$subject \ to \ \sum_{i \in \mathcal{K}_m} P_{BS,i,n} \leq P_{max}^m \ \forall m \in \{1,2,\dots,l\}$$

$$\sum_{i \in \mathcal{K}_r} P_{RN,i,n} \leq \bar{P}_{max}^r \ \forall r \in \{1,2,\dots,R\}$$

where, $\bar{P}_{max}^r$ is the maximum transmit power of the cooperative RNs and P_{max}^m is the maximum transmit power of the cooperative BSs.

In order to find if the optimization problem is concave or convex we have to find the second derivative of the following objective function.

$$f\left(p_{BS,i,n}, p_{RN,i,n}\right) = R_{UE,i,n}^{DF}\left(p_{BS,i,n}, p_{RN,i,n}\right) \tag{42}$$

$$= min\{R_{UE,i,n}^{DF}(1), R_{UE,i,n}^{DF}(2)\}$$

$$= \begin{cases} R_{UE,i,n}^{DF}(1) & if \ R_{UE,i,n}^{DF}(1) \leq R_{UE,i,n}^{DF}(2) \\ R_{UE,i,n}^{DF}(2) & if \ R_{UE,i,n}^{DF}(1) > R_{UE,i,n}^{DF}(2) \end{cases}$$

$$\frac{\partial f\left(p_{BS,i,n}, p_{RN,i,n}\right)}{\partial p_{BS,i,n}} = \tag{43}$$

$$
\begin{cases}
\dfrac{1}{2\cdot ln2}\cdot\dfrac{1}{1+SINR_{BS-RN_{i,n}}}\cdot\dfrac{\left\|\overline{h}_{i,n}w_{i,n}\right\|^2}{\sum_{j\in\mathcal{S}_n,j\neq i}\left\|\overline{h_{i,n}}w_{j,n}\right\|^2 p_{BS,j,n}+\sigma^2} & if\ \ R_{UE,i,n}^{DF}(1)\le R_{UE,i,n}^{DF}(2)\\[4mm]
\dfrac{1}{2\cdot ln2}\cdot\dfrac{1}{1+SINR_{BS-UE_{i,n}}+SINR_{RN-UE_{i,n}}}\cdot\dfrac{\left\|h_{i,n}w_{i,n}\right\|^2}{\sum_{j\in\mathcal{S}_n,j\neq i}\left\|h_{i,n}w_{j,n}\right\|^2 p_{BS,j,n}+\sigma^2} & if\ R_{UE,i,n}^{DF}(1)>R_{UE,i,n}^{DF}(2)
\end{cases}
$$

$$
\frac{\partial f\left(p_{BS,i,n},p_{RN,i.n}\right)}{\partial p_{RN,i,n}}= \tag{44}
$$

$$
\begin{cases}
0 & if\ \ R_{UE,i,n}^{DF}(1)\le R_{UE,i,n}^{DF}(2)\\[4mm]
\dfrac{1}{2\cdot ln2}\cdot\dfrac{1}{1+SINR_{BS-UE_{i,n}}+SINR_{RN-UE_{i,n}}}\cdot\dfrac{\left\|h_{RN,i,n}w_{RN,i,n}\right\|^2}{\sum_{j\in\mathcal{S}_n,j\neq i}\left\|h_{RN,i,n}w_{RN,j,n}\right\|^2 p_{RN,j,n}+\sigma^2} & if\ R_{UE,i,n}^{DF}(1)>R_{UE,i,n}^{DF}(2)
\end{cases}
$$

$$
\frac{\partial^2 f\left(p_{BS,i,n},p_{RN,i,n}\right)}{\partial p_{BS,i,n}}= \tag{45}
$$

$$
\begin{cases}
\dfrac{1}{2\cdot ln2}\cdot\left(\dfrac{\left\|\overline{h}_{i,n}w_{i,n}\right\|^2}{\sum_{j\in\mathcal{S}_n,j\neq i}\left\|\overline{h_{i,n}}w_{j,n}\right\|^2 p_{BS,j,n}+\sigma^2}\right)^2\cdot-\dfrac{1}{\left(1+SINR_{BS-RN_{i,n}}\right)^2} & if\ \ R_{UE,i,n}^{DF}(1)\le R_{UE,i,n}^{DF}(2)\\[6mm]
\dfrac{1}{2\cdot ln2}\cdot\left(\dfrac{\left\|h_{i,n}w_{i,n}\right\|^2}{\sum_{j\in\mathcal{S}_n,j\neq i}\left\|h_{i,n}w_{j,n}\right\|^2 p_{BS,j,n}+\sigma^2}\right)^2\cdot-\dfrac{1}{\left(1+SINR_{BS-UE_{i,n}}+SINR_{RN-UE_{i,n}}\right)^2} & if\ R_{UE,i,n}^{DF}(1)>R_{UE,i,n}^{DF}(2)
\end{cases}
$$

$$
\frac{\partial^2 f\left(p_{BS,i,n},p_{RN,i,n}\right)}{\partial p_{RN,i,n}}= \tag{46}
$$

$$
\begin{cases}
0 & if\ \ R_{UE,i,n}^{DF}(1)\le R_{UE,i,n}^{DF}(2)\\[6mm]
\dfrac{1}{2\cdot ln2}\cdot\left(\dfrac{\left\|h_{RN,i,n}w_{RN,i,n}\right\|^2}{\sum_{j\in\mathcal{S}_n,j\neq i}\left\|h_{RN,i,n}w_{RN,j,n}\right\|^2 p_{RN,j,n}+\sigma^2}\right)^2\cdot-\dfrac{1}{\left(1+SINR_{BS-UE_{i,n}}+SINR_{RN-UE_{i,n}}\right)^2} & if\ R_{UE,i,n}^{DF}(1)>R_{UE,i,n}^{DF}(2)
\end{cases}
$$

From the partial second derivatives of our objective function derived above it is clear that they are negative, thus our function is concave and it has a global maximum.

B. Optimization Problem solution

To solve the maximization problem, I have to define the Lagrange equation.

$$L\left(P_{BS,i,n}, P_{RN,i,n}, \lambda_1, \widetilde{\lambda_1}, \widetilde{\lambda_2}\right) \tag{47}$$

$$= \begin{cases} R_{UE,i,n}^{DF}(1) + \lambda_1\left(\displaystyle\sum_{i\in\mathcal{K}_m} P_{BS,i,n} - P_{max}^m\right) \\[2em] R_{UE,i,n}^{DF}(2) + \widetilde{\lambda_1}\left(\displaystyle\sum_{i\in\mathcal{K}_m} P_{BS,i,n} - P_{max}^m\right) + \widetilde{\lambda_2}\left(\displaystyle\sum_{i\in\mathcal{K}_r} P_{RN,i,n} - \bar{P}_{max}^r\right) \end{cases}$$

Now, I am going to solve for the first Lagragian equation.

$$\frac{\partial L\left(P_{BS,i,n}, P_{RN,i,n}, \lambda_1\right)}{\partial P_{BS,i,n}} = \tag{48}$$

$$\frac{1}{2\cdot ln2}\cdot\frac{1}{1+SINR_{BS-RN_{i,n}}}\cdot\frac{\left\|\bar{h}_{i,n}w_{i,n}\right\|^2}{\sum_{j\in\mathcal{S}_n, j\neq i}\left\|\overline{h_{\iota,n}}w_{j,n}\right\|^2 p_{BS,j,n} + \sigma^2} + \lambda_1 = 0$$

$$\frac{\partial L\left(P_{BS,i,n}, P_{RN,i,n}, \lambda_1\right)}{\partial \lambda_1} = \left(\sum_{i\in\mathcal{K}_m} P_{BS,i,n} - P_{max}^m\right) = 0 \tag{49}$$

Then, $\sum_{i\in\mathcal{K}_m} P_{BS,i,n} = P_{max}^m$.

The powers are find as follows which will depend on λ_1 :

$$\frac{1}{2\cdot ln2}\cdot\frac{1}{1+\dfrac{\left\|\overline{h_{\iota,n}}w_{i,n}\right\|^2 p_{BS,i,n}}{\sum_{j\in\mathcal{S}_n, j\neq i}\left\|\overline{h_{\iota,n}}w_{j,n}\right\|^2 p_{BS,j,n} + \sigma^2}}\cdot\frac{\left\|\bar{h}_{i,n}w_{i,n}\right\|^2}{\sum_{j\in\mathcal{S}_n, j\neq i}\left\|\overline{h_{\iota,n}}w_{j,n}\right\|^2 p_{BS,j,n} + \sigma^2} + \lambda_1$$

$$= 0$$

$$\lambda_1 = -\frac{1}{2\cdot ln2}\cdot\frac{1}{1+\dfrac{\left\|\overline{h_{\iota,n}}w_{i,n}\right\|^2 p_{BS,i,n}}{\sum_{j\in\mathcal{S}_n, j\neq i}\left\|\overline{h_{\iota,n}}w_{j,n}\right\|^2 p_{BS,j,n} + \sigma^2}}\cdot\frac{\left\|\bar{h}_{i,n}w_{i,n}\right\|^2}{\sum_{j\in\mathcal{S}_n, j\neq i}\left\|\overline{h_{\iota,n}}w_{j,n}\right\|^2 p_{BS,j,n} + \sigma^2}$$

$$1+\frac{\left\|\overline{h_{\iota,n}}w_{i,n}\right\|^2 p_{BS,i,n}}{\sum_{j\in\mathcal{S}_n, j\neq i}\left\|\overline{h_{\iota,n}}w_{j,n}\right\|^2 p_{BS,j,n} + \sigma^2} = -\frac{1}{2\cdot ln2}\cdot\frac{\left\|\bar{h}_{i,n}w_{i,n}\right\|^2}{\sum_{j\in\mathcal{S}_n, j\neq i}\left\|\overline{h_{\iota,n}}w_{j,n}\right\|^2 p_{BS,j,n} + \sigma^2}\cdot\frac{1}{\lambda_1}$$

32

$$p_{BS,i,n} = \left[-\frac{1}{2 \cdot ln2} \cdot \frac{\left\| \bar{h}_{i,n} w_{i,n} \right\|^2}{\sum_{j \in \mathcal{S}_n, j \neq i} \left\| \overline{h_{i,n}} w_{j,n} \right\|^2 p_{BS,j,n} + \sigma^2} \cdot \frac{1}{\lambda_1} - 1 \right] \qquad (50)$$

$$\cdot \frac{\sum_{j \in \mathcal{S}_n, j \neq i} \left\| \overline{h_{i,n}} w_{j,n} \right\|^2 p_{BS,j,n} + \sigma^2}{\left\| \overline{h_{i,n}} w_{i,n} \right\|^2}$$

Now, for the second Lagragian equation I will find the partial derivatives.

$$\frac{\partial L\left(P_{BS,i,n}, P_{RN,i,n}, \widetilde{\lambda_1}, \widetilde{\lambda_2}\right)}{\partial P_{BS,i,n}} = \qquad (51)$$

$$\frac{1}{2 \cdot ln2} \cdot \frac{1}{1 + SINR_{BS-UE\,i,n} + SINR_{RN-UE\,i,n}} \cdot \frac{\left\| h_{i,n} w_{i,n} \right\|^2}{\sum_{j \in \mathcal{S}_n, j \neq i} \left\| h_{i,n} w_{j,n} \right\|^2 p_{BS,j,n} + \sigma^2} + \widetilde{\lambda_1} = 0$$

$$\frac{\partial L\left(P_{BS,i,n}, P_{RN,i,n}, \widetilde{\lambda_1}, \widetilde{\lambda_2}\right)}{\partial P_{RN,i,n}} = \qquad (52)$$

$$\frac{1}{2 \cdot ln2} \cdot \frac{1}{1 + SINR_{BS-UE\,i,n} + SINR_{RN-UE\,i,n}} \cdot \frac{\left\| h_{RN,i,n} w_{RN,i,n} \right\|^2}{\sum_{j \in \mathcal{S}_n, j \neq i} \left\| h_{RN,i,n} w_{RN,j,n} \right\|^2 p_{RN,j,n} + \sigma^2}$$

$$+ \widetilde{\lambda_2} = 0$$

$$\frac{\partial L\left(P_{BS,i,n}, P_{RN,i,n}, \widetilde{\lambda_1}, \widetilde{\lambda_2}\right)}{\partial \widetilde{\lambda_1}} = \left(\sum_{i \in \mathcal{K}_m} P_{BS,i,n} - P_{max}^m \right) = 0 \qquad (53)$$

Then, $\sum_{i \in \mathcal{K}_m} P_{BS,i,n} = P_{max}^m$.

$$\frac{\partial L\left(P_{BS,i,n}, P_{RN,i,n}, \widetilde{\lambda_1}, \widetilde{\lambda_2}\right)}{\partial \widetilde{\lambda_2}} = \left(\sum_{i \in \mathcal{K}_r} P_{RN,i,n} - \bar{P}_{max}^r \right) = 0 \qquad (54)$$

Then, $\sum_{i \in \mathcal{K}_r} P_{RN,i,n} = \bar{P}_{max}^r$.

The allocated power now will depend on $\widetilde{\lambda_1}$ & $\widetilde{\lambda_2}$.

$$\frac{1}{2 \cdot ln2} \cdot \frac{1}{1 + \frac{\|h_{i,n}w_{i,n}\|^2 p_{BS,i,n}}{\sum_{j \in \mathcal{S}_n, j \neq i} \|h_{i,n}w_{j.n}\|^2 p_{BS,j,n} + \sigma^2} + \frac{\|h_{RN,i,n}w_{RN,i,n}\|^2 p_{RN,i,n}}{\sum_{j \in \mathcal{S}_n, j \neq i} \|h_{RN,i,n}w_{RN,j,n}\|^2 p_{RN,j,n} + \sigma^2}}$$

$$\cdot \frac{\|h_{i,n}w_{i,n}\|^2}{\sum_{j \in \mathcal{S}_n, j \neq i} \|h_{i,n}w_{j.n}\|^2 p_{BS,j,n} + \sigma^2} + \widetilde{\lambda_1} = 0$$

$$\widetilde{\lambda_1}$$

$$= -\frac{1}{2 \cdot ln2}$$

$$\cdot \frac{1}{1 + \frac{\|h_{i,n}w_{i,n}\|^2 p_{BS,i,n}}{\sum_{j \in \mathcal{S}_n, j \neq i} \|h_{i,n}w_{j.n}\|^2 p_{BS,j,n} + \sigma^2} + \frac{\|h_{RN,i,n}w_{RN,i,n}\|^2 p_{RN,i,n}}{\sum_{j \in \mathcal{S}_n, j \neq i} \|h_{RN,i,n}w_{RN,j,n}\|^2 p_{RN,j,n} + \sigma^2}}$$

$$\cdot \frac{\|h_{i,n}w_{i,n}\|^2}{\sum_{j \in \mathcal{S}_n, j \neq i} \|h_{i,n}w_{j.n}\|^2 p_{BS,j,n} + \sigma^2}$$

$$1 + \frac{\|h_{i,n}w_{i,n}\|^2 p_{BS,i,n}}{\sum_{j \in \mathcal{S}_n, j \neq i} \|h_{i,n}w_{j.n}\|^2 p_{BS,j,n} + \sigma^2} + \frac{\|h_{RN,i,n}w_{RN,i,n}\|^2 p_{RN,i,n}}{\sum_{j \in \mathcal{S}_n, j \neq i} \|h_{RN,i,n}w_{RN,j,n}\|^2 p_{RN,j,n} + \sigma^2}$$

$$= -\frac{1}{2 \cdot ln2} \cdot \frac{\|h_{i,n}w_{i,n}\|^2}{\sum_{j \in \mathcal{S}_n, j \neq i} \|h_{i,n}w_{j.n}\|^2 p_{BS,j,n} + \sigma^2} * \frac{1}{\widetilde{\lambda_1}}$$

$$p_{BS,i,n} = \hspace{4cm} (55)$$

$$\left[-\frac{1}{2 \cdot ln2} \cdot \frac{\|h_{i,n}w_{i,n}\|^2}{\sum_{j \in \mathcal{S}_n, j \neq i} \|h_{i,n}w_{j.n}\|^2 p_{BS,j,n} + \sigma^2} \cdot \frac{1}{\widetilde{\lambda_1}} \right.$$

$$\left. - \frac{\|h_{RN,i,n}w_{RN,i,n}\|^2 p_{RN,i,n}}{\sum_{j \in \mathcal{S}_n, j \neq i} \|h_{RN,i,n}w_{RN,j,n}\|^2 p_{RN,j,n} + \sigma^2} - 1 \right]$$

$$\cdot \left[\frac{\sum_{j \in \mathcal{S}_n, j \neq i} \|h_{i,n}w_{j.n}\|^2 p_{BS,j,n} + \sigma^2}{\|h_{i,n}w_{i,n}\|^2} \right]$$

$$\widetilde{\lambda_2}$$

$$= -\frac{1}{2 \cdot ln2}$$

$$\cdot \frac{1}{1 + \dfrac{\left\|h_{i,n}w_{i,n}\right\|^2 p_{BS,i,n}}{\sum_{j \in \mathcal{S}_n, j \neq i} \left\|h_{i,n}w_{j.n}\right\|^2 p_{BS,j,n} + \sigma^2} + \dfrac{\left\|h_{RN,i,n}w_{RN,i,n}\right\|^2 p_{RN,i,n}}{\sum_{j \in \mathcal{S}_n, j \neq i} \left\|h_{RN,i,n}w_{RN,j,n}\right\|^2 p_{RN,j,n} + \sigma^2}}$$

$$\cdot \frac{\left\|h_{RN,i,n}w_{RN,i,n}\right\|^2}{\sum_{j \in \mathcal{S}_n, j \neq i} \left\|h_{RN,i,n}w_{RN,j,n}\right\|^2 p_{RN,j,n} + \sigma^2}$$

$$1 + \frac{\left\|h_{i,n}w_{i,n}\right\|^2 p_{BS,i,n}}{\sum_{j \in \mathcal{S}_n, j \neq i} \left\|h_{i,n}w_{j.n}\right\|^2 p_{BS,j,n} + \sigma^2} + \frac{\left\|h_{RN,i,n}w_{RN,i,n}\right\|^2 p_{RN,i,n}}{\sum_{j \in \mathcal{S}_n, j \neq i} \left\|h_{RN,i,n}w_{RN,j,n}\right\|^2 p_{RN,j,n} + \sigma^2} =$$

$$-\frac{1}{2 \cdot ln2} \cdot \frac{\left\|h_{RN,i,n}w_{RN,i,n}\right\|^2}{\sum_{j \in \mathcal{S}_n, j \neq i} \left\|h_{RN,i,n}w_{RN,j,n}\right\|^2 p_{RN,j,n} + \sigma^2} \cdot \frac{1}{\widetilde{\lambda_2}}$$

$$p_{RN,i,n} = \left[-\frac{1}{2 \cdot ln2} \cdot \frac{\left\|h_{RN,i,n}w_{RN,i,n}\right\|^2}{\sum_{j \in \mathcal{S}_n, j \neq i} \left\|h_{RN,i,n}w_{RN,j,n}\right\|^2 p_{RN,j,n} + \sigma^2} \cdot \frac{1}{\widetilde{\lambda_2}} \right. \qquad (56)$$

$$\left. -\frac{\left\|h_{i,n}w_{i,n}\right\|^2 p_{BS,i,n}}{\sum_{j \in \mathcal{S}_n, j \neq i} \left\|h_{i,n}w_{j.n}\right\|^2 p_{BS,j,n} + \sigma^2} - 1 \right]$$

$$\cdot \left[\frac{\sum_{j \in \mathcal{S}_n, j \neq i} \left\|h_{RN,i,n}w_{RN,j,n}\right\|^2 p_{RN,j,n} + \sigma^2}{\left\|h_{RN,i,n}w_{RN,i,n}\right\|^2} \right]$$

Then, after finding $p_{RN,i,n}$ and $p_{BS,i,n}$ we can find $\lambda_1, \widetilde{\lambda_1}, \& \widetilde{\lambda_2}$ by using the following two constraints:

$$\sum_{i \in \mathcal{K}_m} P_{BS,i,n} \leq P_{max}^m \ \& \ \sum_{i \in \mathcal{K}_r} P_{RN,i,n} \leq \bar{P}_{max}^r$$

$$\lambda_1 = -\frac{1}{2 \cdot ln2} \cdot \frac{\dfrac{\left\|\bar{h}_{i,n} w_{i,n}\right\|^2}{\sum_{j \in \mathcal{S}_n, j \neq i} \left\|\overline{h_{i,n}} w_{j,n}\right\|^2 p_{BS,j,n} + \sigma^2}}{\left[\dfrac{\left\|\bar{h}_{i,n} w_{i,n}\right\|^2}{\sum_{j \in \mathcal{S}_n, j \neq i} \left\|\overline{h_{i,n}} w_{j,n}\right\|^2 p_{BS,j,n} + \sigma^2}\right] \cdot P_{max}^m + 2} \tag{57}$$

$$\widetilde{\lambda_1} = \tag{58}$$

$$-\frac{1}{ln2}$$

$$\cdot \frac{\dfrac{\left\|h_{i,n} w_{i,n}\right\|^2}{\sum_{j \in \mathcal{S}_n, j \neq i} \left\|h_{i,n} w_{j,n}\right\|^2 p_{BS,j,n} + \sigma^2}}{\left[\dfrac{\left\|h_{i,n} w_{i,n}\right\|^2}{\sum_{j \in \mathcal{S}_n, j \neq i} \left\|h_{i,n} w_{j,n}\right\|^2 p_{BS,j,n} + \sigma^2}\right] \cdot P_{max}^m + \left[\dfrac{\left\|h_{RN,i,n} w_{RN,i,n}\right\|^2}{\sum_{j \in \mathcal{S}_n, j \neq i} \left\|h_{RN,i,n} w_{RN,j,n}\right\|^2 p_{RN,j,n} + \sigma^2}\right] \cdot \bar{P}_{max}^r + 2}$$

$$\widetilde{\lambda_2} = \tag{59}$$

$$-\frac{1}{ln2}$$

$$\cdot \frac{\dfrac{\left\|h_{RN,i,n} w_{RN,i,n}\right\|^2}{\sum_{j \in \mathcal{S}_n, j \neq i} \left\|h_{RN,i,n} w_{RN,j,n}\right\|^2 p_{RN,j,n} + \sigma^2}}{\left[\dfrac{\left\|h_{i,n} w_{i,n}\right\|^2}{\sum_{j \in \mathcal{S}_n, j \neq i} \left\|h_{i,n} w_{j,n}\right\|^2 p_{BS,j,n} + \sigma^2}\right] \cdot P_{max}^m + \left[\dfrac{\left\|h_{RN,i,n} w_{RN,i,n}\right\|^2}{\sum_{j \in \mathcal{S}_n, j \neq i} \left\|h_{RN,i,n} w_{RN,j,n}\right\|^2 p_{RN,j,n} + \sigma^2}\right] \cdot \bar{P}_{max}^r + 2}$$

To find the powers that must be allocated by the BSs and the RNs for the cell-edge UEs, the following algorithm must be done.

Consider interference term = 0

1. Find λ_1 based on equation 57
2. Find $p_{BS,i,n}$ based on equation 50
3. Find $\widetilde{\lambda_1}$ and $\widetilde{\lambda_2}$ based on equation 58 and 59
4. Find $p_{RN,i,n}$ based on equation 56 and through using $p_{BS,i,n}$ and $\widetilde{\lambda_2}$ found previously
5. Then, Find the new $p_{BS,i,n}$ based on equation 55 and through using $p_{RN,i,n}$ and $\widetilde{\lambda_1}$

C. Objective Function Analysis

The simulation of the optimization problem is done per the nth RB. Figure 5.1 below shows $R_{UE,i,n}^{DF}(1)$ for UE1 (k=1, Blue curve) and UE2 (k=2, Red curve). The green curve is the overall rate of UE1 and UE2 (i:e summation of $R_{UE,1,n}^{DF}(1)$ and $R_{UE,2,n}^{DF}(1)$). In the simulation I considered that the power allocated for UE1 by the cooperative BSs is P_{BS_UE1}, and the power allocated for UE1 by the cooperating RNs is P_{RN_UE1}. Then, the power allocated for UE2 by the cooperative BSs is Total power of BS - P_{BS_UE1}, and the power allocated for UE2 by the cooperative RNs is Total power of RN - P_{RN_UE1}.

Moreover, $R_{UE,i,n}^{DF}(1)$ depends on the power allocation at the BS as seen in the equation defined before. Thus, as P_{BS_UE1} increases $R_{UE,1,n}^{DF}(1)$ increases while $R_{UE,2,n}^{DF}(1)$ decreases.
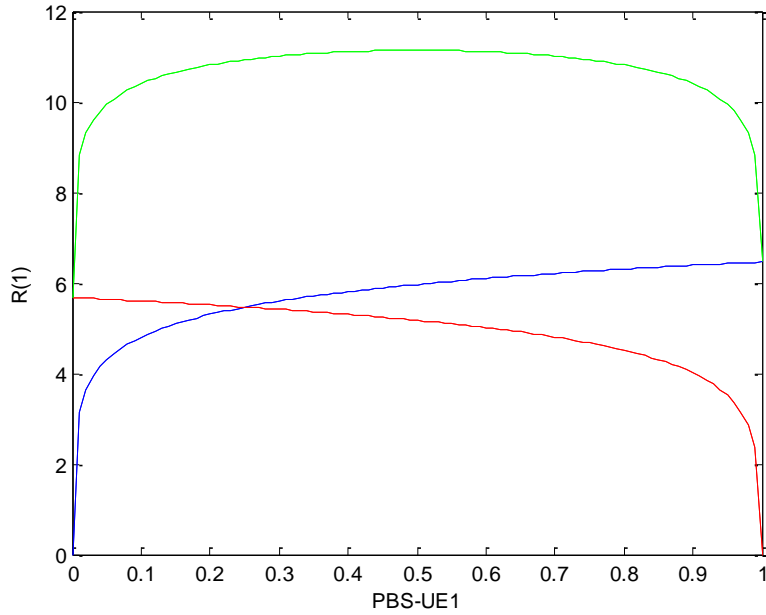

Figure 5.1: Variation of $R_{UE,i,n}^{DF}(1)$ as a function of P_{BS_UE1}

Figure 5.2 shows $R_{UE,1,n}^{DF}(2)$ (i:e for UE1) which depends on the power allocated at the BS and the power allocated at the RNs as seen in the equation before. Figure 5.2 shows that for a specific P_{RN_UE1} if we increase P_{BS_UE1} then $R_{UE,1,n}^{DF}(2)$ will increase accordingly. Moreover, for a specific P_{BS_UE1} if we increase P_{RN_UE1} then $R_{UE,1,n}^{DF}(2)$ will increase accordingly.
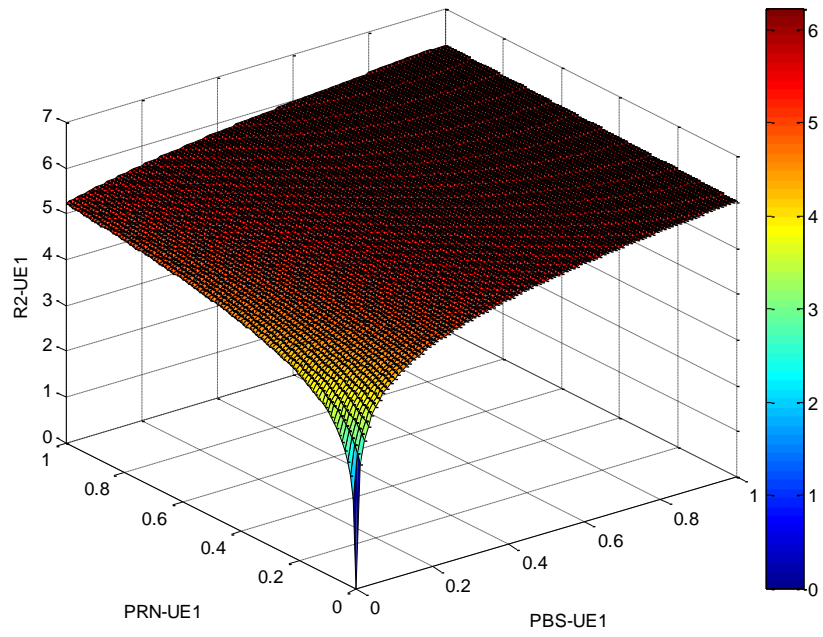
Figure 5.2: Variation of $R_{UE,1,n}^{DF}(2)$ as function of P_{BS_UE1} and P_{RN_UE1}

Then figure 5.3 shows $R_{UE,i,n}^{DF}(p_{BS,i,n}, p_{RN,i,n}) = min\{R_{UE,i,n}^{DF}(1), R_{UE,i,n}^{DF}(2)\}$ for UE1. Which is an increasing function.
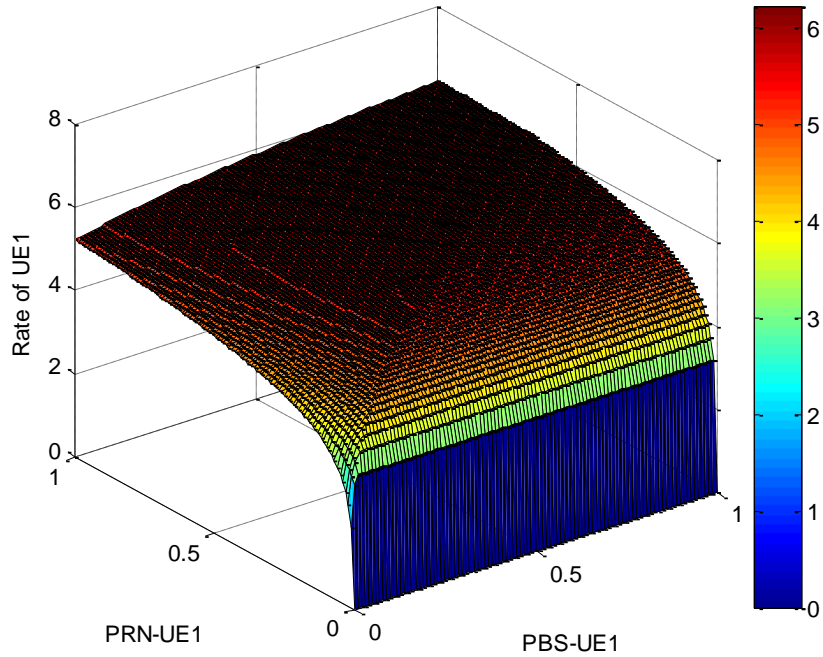

Figure 5.3: Overall rate of UE1 as a function of P_{BS_UE1} and P_{RN_UE1}

Then figure 5.4 shows $R_{UE,k,n}^{DF}(p_{BS,k,n}, p_{RN,k,n}) = min\{R_{UE,k,n}^{DF}(1), R_{UE,k,n}^{DF}(2)\}$ for UE2, which is a decreasing function.
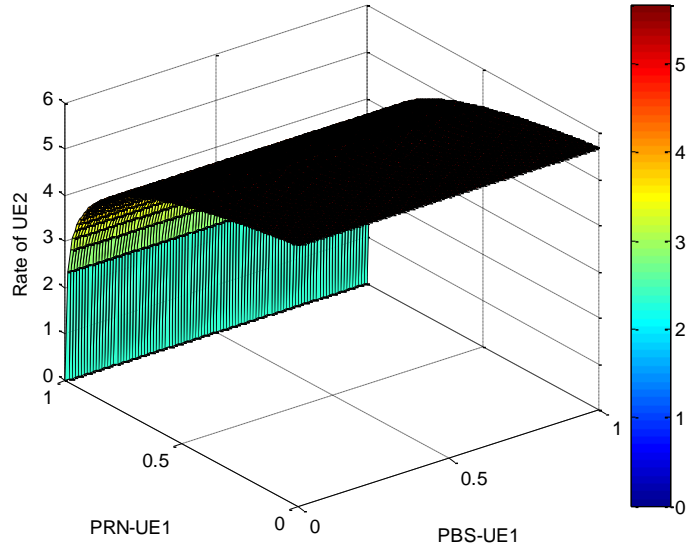

Figure 5.4: Overall rate of UE2 as a function of PBS_UE1 and PRN_UE1

Then figure 5.5 shows the overall rate of our system which is $R_{UE,1,n}^{DF}(p_{BS,i,n}, p_{RN,i,n}) + R_{UE,2,n}^{DF}(p_{BS,i,n}, p_{RN,i,n})$.
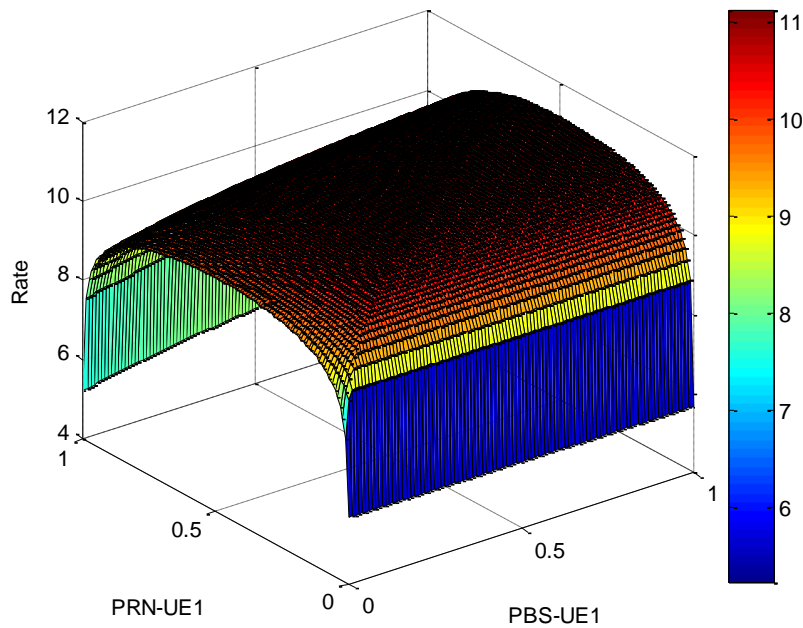

Figure 5.5: Overall rate of our system as a function of PBS_UE1 and PRN_UE1

CHAPTER VI

CONCLUSION

In conclusion, the system proposed in my thesis can make more use of already deployed RNs in the LTE network and have them participate with the BSs to enhance the signal received at the cell edge UEs. Furthermore, our precoding vectors were designed and evaluated using SVD, QRD and SQRD. The simulation results have shown significant performance gains of our system over traditional JP-CoMP under ideal and real channel estimation. Then, I proved that the optimal location of the RNs in my system design can be identified depending on the power ratio between the RN and the BS. I have simulated a real case scenario where the RNs are randomly deployed in the cell and compared the results with the case when the RNs are always at their optimal locations. The results show that when we choose the RNs that must undergo cooperation that are closest to the optimum location, the system will have a very close rate to the case when the optimal RNs are chosen. Finally, the power optimization problem of the system design is a concave problem were a maximum rate can be obtained for a specific power allocation at the BSs and the RNs.

BIBLIOGRAPHY

[1] Ericsson (2011). "LTE: an introduction" Retrieved from:"http://www.ericsson.com/res/docs/2011/lte_an_introduction.pdf

[2] M. Dehghani, K.Arshad, "LTE-advanced, and the way forward," *14th Intl. Symp. on Comm. and Information Technologies (ISCIT)*, 2014.

[3] E. Pateromichelakis, M. Shariat, A. ul Quddus, R. Tafazolli, "On the Evolution of Multi-Cell Scheduling in 3GPP LTE / LTE-A," *IEEE Comm. Surveys & Tutorials*, v. 15, n. 2, pp. 701-717, 2013

[4] 3GPP TR 36.819, "Coordinated multi-point operation for LTE physical layer aspects (Release 11)", v. 11.2.0, September, 2013.

[5] A. Lo and P. Guan, "Joint Cooperative Shared Relaying and Multipoint Coordination for Network MIMO in 3GPP LTE-Advanced Multihop Cellular Networks, Recent Developments in Mobile Comm. - A Multidisciplinary Approach", Dr Juan P. Maícas (Ed.), 2011.

[6] W. Zirwas, U. Zeeshan, M. Grieger, "Cooperative feeder links for relay enhanced networks", *18th European Wireless Conference*, pp. 1-8, April 2012

[7] J.A. Aldhaibani, A. Yahya, R.B. Ahmad, N. Omar, Z.G. Ali, "Effect of relay location on two-way DF and AF relay for multi-user system in LTE-A cellular networks", *IEEE in Business Engineering and Industrial Applications Colloquium (BEIAC)*, pp.380-385, April 2013

[8] J-W. Kwon, K-H. Park, Y-C. Ko, H-C. Yang, "Cooperative Joint Precoding in a Downlink Cellular System with Shared Relay: Design and Performance Evaluation", *IEEE Transactions on Wireless Comm.*, v.11, n.10, pp. 3462-3473, 2012

[9] T. Lakshmana, C. Botella, and T. Svensson, "Partial joint processing with efficient backhauling using particle swarm optimization", *EURASIP Journal on Wireless Comm. and Net.*, v. 1, pp. 1-18. 2012

[10] Y.L. Wei Zhou, D. Z. Yue Sun, "A Novel Network Coding Multi-User Coordinated Multipoint Downlink Transmission Scheme," in Vehicular Technology Conference (VTC Fall), 2012 IEEE , vol., no., pp.1-5, 3-6 Sept. 2012

[11] J. Jin, Q. Wang, G. Liu, H. Yang; Y. Wang; X. Zhang, "A Novel Cooperative Multi-Cell MIMO Scheme for the Downlink of LTE-Advanced System," Comm. Workshops, 2009. ICC Workshops 2009. IEEE Intl. Conference on, pp.1,5, June 2009

[12] W. Fu, L. Ma, C. Wang, Q. Kong, W. Tian, "The Inter-cell Interference Suppression Algorithm Based on the JP-CoMP and Performance Simulation," Advanced Information Networking and Applications Workshops (WAINA), 2013 27th Intl. Conference on, pp.528,533, March 2013

[13] S. Scott, J. Leinonen, P. Pirinen, J. Vihriala, V. Van Phan, M. Latva-aho, "A Cooperative Moving Relay Node System Deployment in a High Speed Train," in Vehicular Technology Conference (VTC Spring), 2013 IEEE 77th , vol., no., pp.1-5, 2-5 June 2013

[14] M.A.L. Sarker, M.H. Lee, "Interference alignment and cancellation over the LTE-A based on coordinated multi-point system," in Ultra Modern TeleComm. and Control Systems and Workshops (ICUMT), 2012 4th Intl. Congress on , vol., no., pp.516-522, 3-5 Oct. 2012

[15] C.L. Wu; T.N. Lin, H.F. Liu, Z.Y. Chen, "On relay assignment strategy in wireless cellular environment," *Intl. Conf. Comp., Net. and Comm. (ICNC)*, pp. 698-703, Feb. 2014

[16] M. Khan, M.H. Lee, "Zero-forcing beamforming with block diagonalization scheme for Coordinated Multi-Point transmission," *18th Asia-Pacific Conf. Comm. (APCC)*, pp. 152-156, Oct. 2012

[17] E. Hossain, V.K. Bhargava, & G. P. Fettweis, (2012). Green radio communication networks. Cambridge University Press

[18] H. Sun, W. Fang, L. Yang, "A Novel Precoder Design for Coordinated Multipoint Downlink Transmission," IEEE Vehicular Technology Conference (VTC Spring), pp. 1-5, May 2011

[19] C.H. Lin, P.Y. Tsai, "A reduced-complexity multi-user MIMO precoding scheme with sorted-QR decomposition and block-based power allocation," *Intl. Conf. ITS TeleComm. (ITST)*, pp. 658-662, Aug. 2011

[20] R. S. Kshetrimayum EC635. Cellular concepts [Online]. Available: http://www.iitg.ernet.in/engfac/krs/public_html/lectures/ee635/A3.pdf

[21] S. Lagen, A. Agustin, & J.Vidal, (2013). "Network-MIMO for downlink in-band relay transmissions", *EURASIP Journal on Wireless Comm. and Net.*, 2013(1), 1-15.

[22] M. Yang, O.S. Shin, Y. Shin, H. Kim, "Inter-cell interference management using multi-cell Shared Relay Nodes in 3GPP LTE-Advanced networks", *Wireless Comm. and Net. Conf. (WCNC)*, pp. 3579-3584, April 2013

[23] T. Okamawari, Liang Zhang, A. Nagate, H. Hayashi, T. Fujii, "Design of Control Architecture for Downlink CoMP Joint Transmission with Inter-eNB Coordination in Next Generation Cellular Systems," Vehicular Technology Conference (VTC Fall), 2011 IEEE , pp.1,5, Sept. 2011

[24] Bing Luo; Qimei Cui; Xiaofeng Tao; Alexis, D., "On the optimal power allocation for coordinated wireless backhaul in OFDM-based relay systems," Communications (ICC), 2013 IEEE International Conference on , pp.5625,5629, June 2013